

CERN-EP-2023-148
24 July 2023

Measurement of Non-prompt D^0 -meson Elliptic Flow in Pb–Pb Collisions at $\sqrt{s_{\text{NN}}} = 5.02 \text{ TeV}$

ALICE Collaboration*

Abstract

The elliptic flow (v_2) of D^0 mesons from beauty-hadron decays (non-prompt D^0) was measured in midcentral (30–50%) Pb–Pb collisions at a centre-of-mass energy per nucleon pair $\sqrt{s_{\text{NN}}} = 5.02 \text{ TeV}$ with the ALICE detector at the LHC. The D^0 mesons were reconstructed at midrapidity ($|y| < 0.8$) from their hadronic decay $D^0 \rightarrow K^- \pi^+$, in the transverse momentum interval $2 < p_T < 12 \text{ GeV}/c$. The result indicates a positive v_2 for non-prompt D^0 mesons with a significance of 2.7σ . The non-prompt D^0 -meson v_2 is lower than that of prompt non-strange D mesons with 3.2σ significance in $2 < p_T < 8 \text{ GeV}/c$, and compatible with the v_2 of beauty-decay electrons. Theoretical calculations of beauty-quark transport in a hydrodynamically expanding medium describe the measurement within uncertainties.

1 Introduction

A phase of matter made of deconfined quarks and gluons, called the quark–gluon plasma (QGP), is created in ultrarelativistic heavy-ion collisions, as supported by several measurements at the SPS, RHIC, and LHC particle accelerators [1–9]. The QGP formed in such extreme conditions is considered to be a nearly perfect fluid [10]. Heavy quarks (charm and beauty), mostly produced via hard partonic scattering processes on a timescale shorter than the QGP formation time [11, 12], are effective probes of the properties and dynamics of the QGP. They interact with the medium constituents, losing energy via radiative and collisional processes [13]. The significant suppression of charm- and beauty-hadron production yields at intermediate and high transverse momentum ($p_T > 6 \text{ GeV}/c$) observed in heavy-ion collisions at both RHIC [14–18] and LHC [19–33], compared to appropriately scaled yields from proton–proton (pp) collisions, indicates a substantial energy loss of heavy quarks in the QGP.

The azimuthal anisotropy in momentum space of final-state hadrons acts as an additional observable to probe the properties of the QGP. In non-central nucleus–nucleus collisions, the spatial anisotropy in the initial matter distribution due to the asymmetry of the nuclear overlap region is transferred to the final-state particle momentum distribution via multiple collisions, a phenomenon referred to as anisotropic flow [34, 35]. The anisotropic flow is quantified by the harmonic coefficients $v_n = \langle \cos[n(\varphi - \Psi_n)] \rangle$ of the Fourier expansion of the particle azimuthal angle (φ) relative to the collision symmetry planes with angles Ψ_n for the n^{th} harmonic. The second harmonic, v_2 , also known as elliptic flow, is the largest coefficient in non-central heavy-ion collisions. At low p_T ($p_T < 6 \text{ GeV}/c$), the heavy-flavour v_2 can help to quantify the extent to which charm and beauty quarks participate in the collective expansion of the medium [36] and the fraction of heavy quarks hadronising via recombination with light quarks in the QGP medium in the intermediate p_T region ($6 < p_T < 10 \text{ GeV}/c$) [37, 38]. In addition, at high p_T ($p_T > 10 \text{ GeV}/c$), the v_2 of heavy-flavour hadrons can constrain the path-length dependence of energy loss in the medium for heavy quarks [39, 40].

D mesons and charm-hadron decay leptons show a positive v_2 in nucleus–nucleus collisions at both RHIC [14, 41–43] and LHC [44–53] energies. The comparison of experimental measurements with theoretical models indicates that charm quarks participate in the collective expansion of the medium, and both collisional processes and the hadronisation of charm quarks via coalescence with light quarks are important to describe the observed elliptic flow [54–63]. In particular, the D-meson v_2 has a magnitude similar to the v_2 of charged pions for $3 < p_T < 6 \text{ GeV}/c$, suggesting that low- p_T charm quarks have a relaxation time comparable to the QGP lifetime [64]. Due to their higher mass, beauty quarks are unlikely to reach thermalisation in the medium, therefore their azimuthal anisotropy can give further insight into the interactions of heavy quarks with the medium [65–68]. The experimental information is still poor for the beauty-hadron v_2 at low momentum. The elliptic flow of J/ψ mesons originating from beauty-hadron decays (non-prompt) measured by the CMS and ATLAS Collaborations is consistent with zero within large uncertainties for $p_T > 3 \text{ GeV}/c$ [69, 70]. The v_2 of leptons from beauty-hadron decays measured by ALICE and ATLAS is found to be positive [71, 72]. However, due to the small lepton masses, correlations between the kinematic variables (p_T and direction) of the beauty hadrons and the decay leptons are broad. This is improved when choosing a decay into a heavier particle. A measurement of the non-prompt D⁰-meson v_2 has been recently submitted for publication by CMS [73].

In this letter, the measurement of the non-prompt D⁰-meson v_2 at midrapidity ($|y| < 0.8$) in Pb–Pb collisions at a centre-of-mass energy per nucleon pair $\sqrt{s_{\text{NN}}} = 5.02 \text{ TeV}$ with the ALICE detector is reported. The D⁰-meson v_2 is measured with the Scalar Product (SP) method [74, 75] in midcentral collisions (30–50% centrality class). The non-prompt D⁰-meson v_2 is extracted and compared with previous measurements of the prompt non-strange D-meson v_2 (average of D⁰, D⁺, and D^{*+}) and the v_2 of electrons from beauty-hadron decays, as well as with theoretical models based on beauty-quark transport in the QGP.

2 Experimental Apparatus and Data Analysis

A description of the ALICE detector and its performance can be found in Refs. [9, 76, 77]. The main detectors used for this analysis are the Inner Tracking System (ITS) [78] for track and vertex reconstruction, the Time Projection Chamber (TPC) [79] for track reconstruction and particle identification (PID) via the measurement of the specific energy loss, and the Time-Of-Flight (TOF) [80] detector for PID via the measurement of the particle flight time from the interaction point to the detector. These detectors are located inside a large solenoidal magnet providing a magnetic field of up to 0.5 T parallel to the LHC beam direction and cover the pseudorapidity interval $|\eta| < 0.9$. A minimum-bias interaction trigger was used, requiring coincident signals in the V0A and V0C detectors [81], two scintillator arrays covering the full azimuth in the pseudorapidity intervals $2.8 < \eta < 5.1$ (V0A) and $-3.7 < \eta < -1.7$ (V0C). An online selection based on the V0 signal amplitudes was also applied in order to enhance the sample of midcentral collisions as an additional trigger class. Background events from beam–gas interactions were rejected offline using the timing information provided by the V0 and the neutron Zero-Degree Calorimeter (ZDC) [82]. Events used in the analysis were required to have a primary vertex reconstructed within $\pm 10 \text{ cm}$ from the nominal interaction point along the beam axis. Centrality intervals for events were defined in terms of percentiles of the hadronic Pb–Pb cross section based on the signal amplitude of the V0 detectors [83]. After the aforementioned selections, a sample of about 85×10^6 events in the 30–50% centrality class was utilised for further analysis, corresponding to an integrated luminosity of $\mathcal{L}_{\text{int}} \simeq 56 \mu\text{b}^{-1}$ [84].

The D⁰ mesons and their charge conjugates were reconstructed via the hadronic decay channel $D^0 \rightarrow K^- \pi^+$ with branching ratio $\text{BR} = (3.947 \pm 0.030)\%$ [85]. The D⁰-meson candidates were selected combining pairs of tracks with opposite charge signs, each with $p_T > 0.3 \text{ GeV}/c$ and $|\eta| < 0.8$. The selection criteria require at least 70 (out of 159) associated space points in the TPC, a minimum of two (out of six) measured clusters in the ITS, with at least one in either of the two innermost layers, and a fit quality $\chi^2/\text{ndf} < 1.25$ in the TPC. These track selection criteria reduce the D⁰-meson acceptance in rapidity, which falls steeply to zero for $|y| > 0.5$ at low p_T and for $|y| > 0.8$ for $p_T > 5 \text{ GeV}/c$. Thus, a fiducial acceptance selection $|y| < y_{\text{fid}}(p_T)$ was applied to grant a uniform acceptance inside the rapidity range considered. The $y_{\text{fid}}(p_T)$ value was defined as a second-order polynomial function, increasing from 0.5 to 0.8 in $0 < p_T < 5 \text{ GeV}/c$, and as a constant term, $y_{\text{fid}} = 0.8$, for $p_T > 5 \text{ GeV}/c$.

A machine-learning approach with multi-class classification based on Boosted Decision Trees (BDT) was adopted to simultaneously suppress the large combinatorial background and separate the contributions of prompt and non-prompt D⁰ mesons. The implementation of the BDT algorithm provided by the XGBoost [86] library was employed. Samples of prompt and non-prompt D⁰ mesons for the BDT training were obtained from Monte Carlo (MC) samples, which simulated the Pb–Pb events at $\sqrt{s_{\text{NN}}} = 5.02 \text{ TeV}$ with the HIJING v1.383 generator [87]. Additional c̄ or b̄ quark pairs were injected in each simulated event using the PYTHIA 8.243 event generator [88, 89] (Monash 2013 tune [90]) to enrich the MC sample of prompt and non-prompt D⁰-meson signals. The generated particles were transported through the experimental apparatus using the GEANT3 transport package [91]. Samples for the combinatorial background were obtained from candidates in the sideband region in the data, i.e. $5\sigma < |\Delta M| < 9\sigma$ in the invariant mass distribution, where ΔM is the difference between the invariant mass and the mean of signal distribution, and σ is the invariant-mass resolution. Before the training, loose selections on kinematic and topological variables were applied to the D⁰-meson candidates to reduce the computation time. The training variables provided to the BDTs were mainly based on the displacement of the D⁰ decay vertex from the primary vertex of the collision. These included the impact parameter of the D⁰-meson daughter tracks, the distance between the D⁰-meson decay vertex and the primary vertex, and the cosine of the pointing angle between the D⁰-meson candidate line of flight (the vector connecting the primary and secondary vertices) and its reconstructed momentum vector, as well as the PID information of the decay tracks. A detailed description of the training procedure is reported

in Ref. [92]. Independent BDTs were trained in the different p_{T} intervals of the analysis. Subsequently, the BDTs were applied to the experimental data sample to obtain the BDT scores related to the candidate probability to be a non-prompt D⁰ meson or to belong to the combinatorial background. Selections were applied on the scores to reduce the large combinatorial background and to obtain different fractions of non-prompt D⁰ candidates ($f_{\text{non-prompt}}$). The D⁰-meson v_2 coefficient was measured with the Scalar Product (SP) method [74, 75, 93],

$$v_2\{\text{SP}\} = \langle\langle \mathbf{u}_2 \cdot \frac{\mathbf{Q}_2^{\text{V0C}*}}{M^{\text{V0C}}} \rangle\rangle / \sqrt{\frac{\langle \frac{\mathbf{Q}_2^{\text{V0C}}}{M^{\text{V0C}}} \cdot \frac{\mathbf{Q}_2^{\text{V0A}*}}{M^{\text{V0A}}} \rangle \langle \frac{\mathbf{Q}_2^{\text{V0C}}}{M^{\text{V0C}}} \cdot \frac{\mathbf{Q}_2^{\text{TPC}*}}{M^{\text{TPC}}} \rangle}{\langle \frac{\mathbf{Q}_2^{\text{V0A}}}{M^{\text{V0A}}} \cdot \frac{\mathbf{Q}_2^{\text{TPC}*}}{M^{\text{TPC}}} \rangle}} = \langle\langle \mathbf{u}_2 \cdot \frac{\mathbf{Q}_2^{\text{V0C}*}}{M^{\text{V0C}}} \rangle\rangle / R_2, \quad (1)$$

where $\mathbf{u}_2 = e^{i2\phi_{D^0}}$ is the unit flow vector of the D⁰-meson candidate with azimuthal angle ϕ_{D^0} . \mathbf{Q}_2^k and M^k are the subevent 2nd harmonic flow vector and multiplicity for the subevent k , respectively. The denominator, called the resolution (R_2), is calculated with the formula introduced in Ref. [75], where the three subevents are defined by the particles measured in the V0C, V0A, and TPC detectors, respectively. For the TPC detector, the azimuthal angles of charged tracks reconstructed with $|\eta| < 0.8$ and the number of measured tracks were used to calculate the Q_2 vector and M . For the V0A and V0C detectors, the Q_2 vectors were calculated from the azimuthal distribution of the energy deposition in the detector scintillators and M is the sum of the amplitudes measured in each channel [52]. The Q_2 vectors are recalibrated using a recentering procedure [94] to correct for effects of non-uniform acceptance. The nonflow effects are suppressed by the pseudorapidity gaps between the TPC, V0A, and V0C detectors [95]. The single bracket $\langle \rangle$ in Eq. 1 refers to an average over all the events, while the double brackets $\langle\langle \rangle\rangle$ denote the average over all particles in the considered p_{T} interval and all events. The R_2 is extracted as a function of the collision centrality. The centrality-integrated R_2 value is 0.0438 for the 30–50% centrality class.

The D⁰-meson v_2 cannot be measured directly using Eq. 1 since D⁰ mesons cannot be identified on a particle-by-particle basis. Therefore, a simultaneous fit to the invariant-mass spectrum and the v_2 distribution as a function of the invariant mass ($M_{K\pi}$) was performed for D⁰ candidates in each p_{T} interval, in order to measure the raw yields and the v_2 coefficients. The measured total elliptic flow coefficient, v_2^{tot} , can be written as a weighted sum of the v_2 of the D⁰-meson candidates (v_2^{sig}), and that of background (v_2^{bkg}) [96] as

$$v_2^{\text{tot}}(M_{K\pi}) = v_2^{\text{sig}} \frac{N^{\text{sig}}}{N^{\text{sig}} + N^{\text{bkg}}}(M_{K\pi}) + v_2^{\text{bkg}}(M_{K\pi}) \frac{N^{\text{bkg}}}{N^{\text{sig}} + N^{\text{bkg}}}(M_{K\pi}), \quad (2)$$

where N^{sig} and N^{bkg} are the raw signal and background yields, respectively. The fit function for the D⁰-candidate invariant-mass distribution was composed of a Gaussian term to describe the signal and an exponential distribution for the background. The contribution of signal candidates with the reflected K– π mass assignment was taken into account with an additional term, which is small thanks to the good PID capability. It was parameterised by fitting the simulated invariant-mass distribution with a double Gaussian function. To improve the stability of the fits, the widths of the signal peaks were fixed to the values extracted from the fits of the invariant-mass distributions in the prompt enhanced sample, given the naturally larger abundance of prompt compared to non-prompt candidates. In the simultaneous fit, the v_2 parameter for the candidates with wrong K– π mass assignment was set to be equal to v_2^{sig} , provided that the origin of these candidates are real D⁰ mesons. The v_2^{sig} was measured from the fit to the v_2^{tot} distribution with the function of Eq. 2, where v_2^{bkg} is a linear as a function of $M_{K\pi}$ for $p_{\text{T}} > 3$ GeV/ c . For $p_{\text{T}} < 3$ GeV/ c , a second-order polynomial function was used to parametrise $v_2^{\text{bkg}}(M_{K\pi})$. Figure 1 shows an example of the simultaneous fit to the invariant-mass spectrum and v_2^{tot} as a function of $M_{K\pi}$ with low (left panel) and high (right panel) non-prompt D⁰-meson candidate BDT score selections in $3 < p_{\text{T}} < 4$ GeV/ c in the 30–50% centrality class.

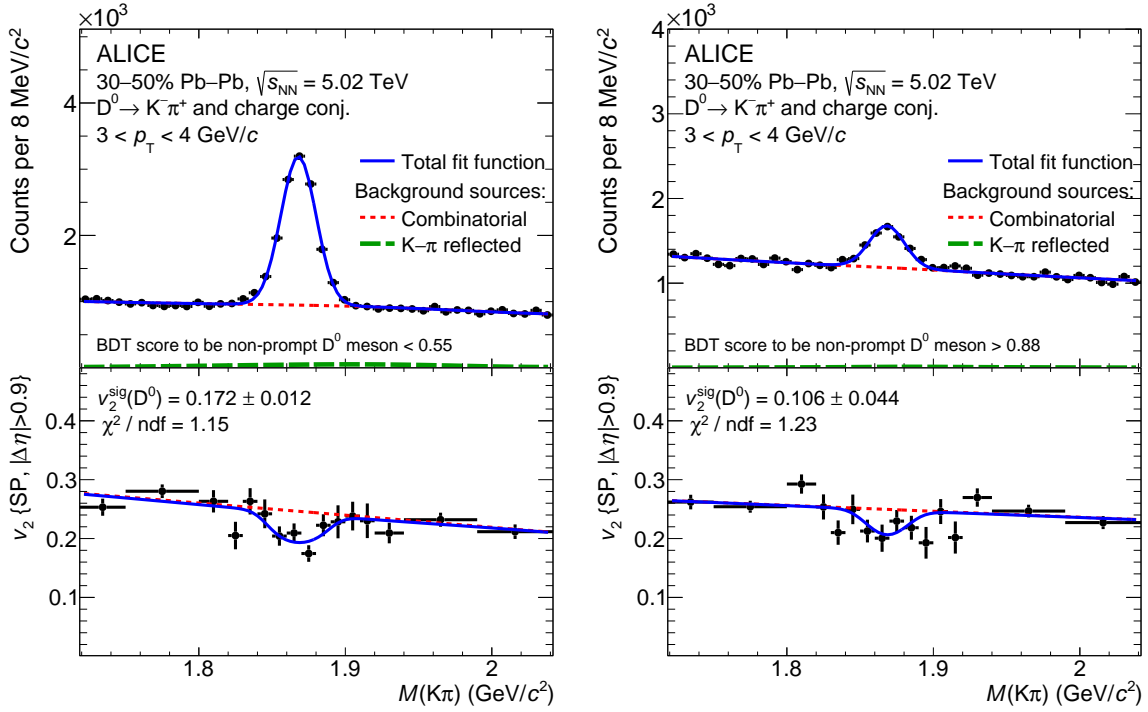


Figure 1: Simultaneous fits of the invariant-mass distribution and $v_2^{\text{tot}}(M_{K\pi})$ of D^0 mesons in $3 < p_T < 4$ GeV/c. Left panel: fits using D^0 -meson candidates with low probability to be a non-prompt D^0 meson. Right panel: fits using D^0 -meson candidates with high probability to be a non-prompt D^0 meson. The corresponding BDT score selection for the measured raw yield is reported. The blue lines, the dotted red curves, and the green solid lines represent the total fit function, the combinatorial-background fit function, and the contribution of the reflected signal, respectively.

The reconstructed D^0 -meson signals are a mixture of prompt and non-prompt D^0 mesons. The v_2^{sig} is therefore a linear combination of prompt (v_2^{prompt}) and non-prompt ($v_2^{\text{non-prompt}}$) contributions, which can be expressed as

$$v_2^{\text{sig}} = (1 - f_{\text{non-prompt}})v_2^{\text{prompt}} + f_{\text{non-prompt}}v_2^{\text{non-prompt}}, \quad (3)$$

where $f_{\text{non-prompt}}$ is estimated as a function of p_T with a data-driven method, which is based on the construction of data samples with different abundances of prompt and non-prompt candidates. A set of raw yields Y_i (index i refers to a given selection on the BDT scores) can be obtained by varying the selection on the BDT score, which is related to the candidate probability to be a non-prompt D^0 meson. These raw yields are related to the corresponding acceptance times efficiency ($\text{Acc} \times \epsilon$) of prompt and non-prompt D^0 mesons according to the equation

$$(\text{Acc} \times \epsilon)_i^{\text{prompt}} N_{\text{prompt}} + (\text{Acc} \times \epsilon)_i^{\text{non-prompt}} N_{\text{non-prompt}} - Y_i = \delta_i, \quad (4)$$

where δ_i represents a residual that accounts for the equation not summing exactly to 0 due to the uncertainties on Y_i , $(\text{Acc} \times \epsilon)_i^{\text{non-prompt}}$, and $(\text{Acc} \times \epsilon)_i^{\text{prompt}}$. By applying at least two different BDT selections and extracting the yields, the corrected yields of prompt (N_{prompt}) and non-prompt ($N_{\text{non-prompt}}$) D^0 mesons can be obtained from Eq. 4 via a χ^2 minimisation. More details can be found in Ref. [92]. The left panel of Fig. 2 shows an example of the raw-yield distributions as a function of the minimum non-prompt D^0 -meson BDT score threshold used in such a χ^2 -minimisation procedure in $3 < p_T < 4$ GeV/c for the 30–50% centrality class. The raw yield decreases with the increasing minimum threshold for the

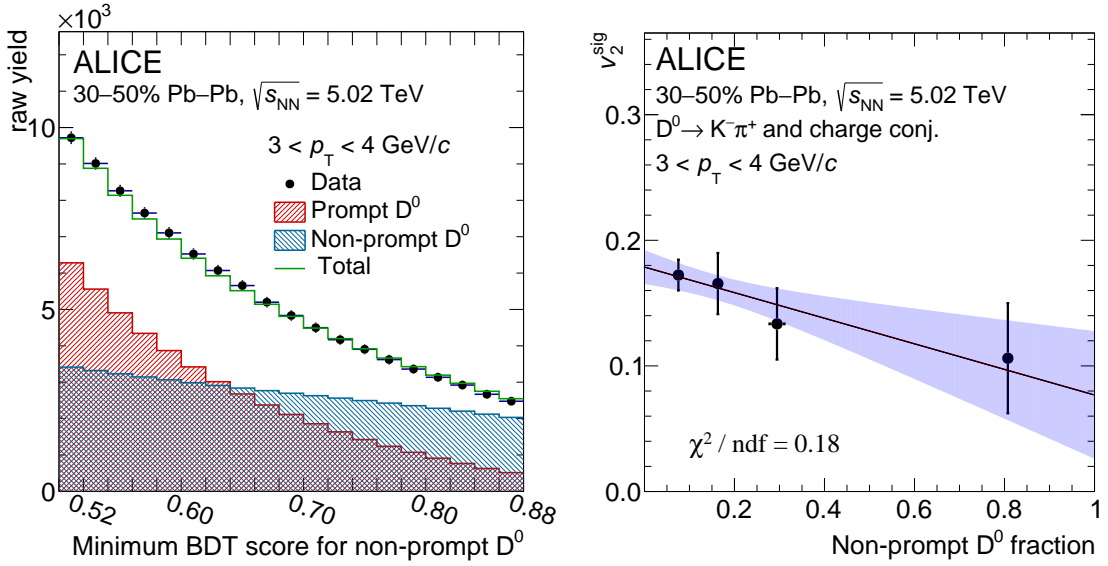


Figure 2: Left panel: example of the raw-yield distribution as a function of the minimum non-prompt D⁰-meson BDT score threshold to determine the non-prompt D⁰-meson fraction in $3 < p_{\text{T}} < 4 \text{ GeV}/c$. Right panel: v_2^{sig} as a function of $f_{\text{non-prompt}}$ in $3 < p_{\text{T}} < 4 \text{ GeV}/c$. The blue band represents the 1σ confidence interval obtained from the linear fit.

score to be a non-prompt D⁰ meson, corresponding to an increasing non-prompt D⁰-meson fraction. The prompt and non-prompt components of the raw yields for each BDT-based selection obtained from the χ^2 -minimisation approach, $(\text{Acc} \times \epsilon)_i^{\text{prompt}} \times N_{\text{prompt}}$ and $(\text{Acc} \times \epsilon)_i^{\text{non-prompt}} \times N_{\text{non-prompt}}$, are shown in the histograms with red and blue colour, respectively, and their sum is reported by the green line. The values of $N_{\text{non-prompt}}$ and N_{prompt} can be used to estimate the non-prompt D⁰-meson fraction in the raw yield for any set of selections i using

$$f_{\text{non-prompt}}^i = \frac{(\text{Acc} \times \epsilon)_i^{\text{non-prompt}} N_{\text{non-prompt}}}{(\text{Acc} \times \epsilon)_i^{\text{non-prompt}} N_{\text{non-prompt}} + (\text{Acc} \times \epsilon)_i^{\text{prompt}} N_{\text{prompt}}}. \quad (5)$$

The v_2^{sig} was determined for three or four non-overlapping intervals of BDT score to be non-prompt D⁰ mesons, depending on the number of candidates in each p_{T} interval. The result was extrapolated to $f_{\text{non-prompt}} = 0$ and $f_{\text{non-prompt}} = 1$ using a linear fit according to Eq. 3 in order to estimate the v_2 values for prompt and non-prompt D⁰ mesons, respectively. A similar approach was adopted in Ref. [97]. The right panel of Fig. 2 shows the linear fit of v_2^{sig} as a function of $f_{\text{non-prompt}}$ in $3 < p_{\text{T}} < 4 \text{ GeV}/c$. The blue band represents the 1σ confidence interval obtained from the linear fit, which is considered as the statistical uncertainty of the v_2^{sig} . As a crosscheck about the correlation of the statistical uncertainties on v_2^{sig} between different values of $f_{\text{non-prompt}}$, the statistical uncertainty was also calculated with the Jackknife method [98] and found to be consistent with the fit method.

3 Systematic Uncertainties

Four major sources of systematic uncertainties were considered for the measurement of the non-prompt D⁰-meson v_2 : (i) the signal extraction from the invariant-mass and v_2^{tot} distributions; (ii) the non-prompt fraction estimation; (iii) the D-meson p_{T} shape in the simulation; and (iv) the centrality dependence of the SP denominator (R_2). All sources of systematic uncertainties were treated as uncorrelated and added in quadrature to obtain the total systematic uncertainties. Table 1 summarises the estimated values of the systematic uncertainties for each p_{T} interval.

Table 1: Summary of the systematic uncertainties on the measurement of the non-prompt D⁰-meson v_2 . The ranges of the uncertainties are quoted as absolute uncertainties, except those on the R_2 as relative uncertainty.

| p_{T} (GeV/ c) | 2–3 | 3–4 | 4–5 | 5–6 | 6–8 | 8–12 |
|--|-------|-------|-------|-------|-------|-------|
| Signal extraction | 0.011 | 0.012 | 0.011 | 0.011 | 0.012 | 0.013 |
| Non-prompt fraction estimation | 0.005 | 0.002 | 0.002 | 0.001 | 0.001 | 0.001 |
| MC D-meson p_{T} distribution | 0.004 | 0.004 | 0.002 | 0.001 | 0.001 | 0.001 |
| R_2 determination | 0.5% | 0.5% | 0.5% | 0.5% | 0.5% | 0.5% |

The systematic uncertainty of the signal extraction from the invariant-mass and v_2^{tot} distributions is due to a possible imperfect modelling of the signal and background distributions. It was evaluated by repeating the simultaneous fit with different configurations. In particular, the fit range, signal width within the statistical uncertainties obtained with prompt enhanced sample, and background fit functions used for the invariant-mass and v_2^{tot} distributions were varied. The systematic uncertainty was defined as the RMS of the distribution of the resulting $v_2^{\text{non-prompt}}$ obtained from all these variations. The second source of systematic uncertainty arises from the uncertainty on the determination of the $f_{\text{non-prompt}}$ of D⁰ mesons with the minimisation method described in Section 2. In this method, the raw yields and the efficiencies obtained with several sets of selections are used in order to extract the prompt and non-prompt components. It is therefore sensitive to possible imperfections of the data description in the MC simulations. They were therefore evaluated by using alternative sets of selections for the aforementioned χ^2 -minimisation approach [92]; the RMS of the resulting $v_2^{\text{non-prompt}}$ distribution was considered as the systematic uncertainty. The systematic effects due to possible differences between the real and simulated p_{T} spectra were estimated by applying different weights to the p_{T} distributions of prompt D⁰ mesons and of the parent beauty hadrons in the case of non-prompt D⁰ mesons. In the default analysis procedure, the weights were defined to match the shape given by FONLL in pp collisions [99, 100] multiplied by the nuclear modification factor (R_{AA}) prediction from the TAMU model [55]. The FONLL spectrum multiplied by the R_{AA} from the LIDO model [101] was used as an alternative shape for the systematic evaluation. The effect due to flow-related modifications of the parent beauty-hadron p_{T} spectra was found to be negligible with respect to the assigned p_{T} -shape systematic uncertainty. The contribution of the SP denominator R_2 to the systematic uncertainty is due to the centrality dependence. It was evaluated as the difference of the centrality-integrated R_2 values with those obtained from weighted average R_2 values in narrow centrality intervals using the D⁰-meson yields as weights [52].

4 Results

The measured non-prompt D⁰-meson elliptic flow at midrapidity ($|y| < 0.8$) in the 30–50% centrality class is shown in Fig. 3 as a function of p_{T} . The weighted mean of the non-prompt D⁰-meson v_2 in the measured p_{T} range ($2 < p_{\text{T}} < 12$ GeV/ c) is 2.7σ above 0. No significant p_{T} dependence of the v_2 is observed. The results obtained are compatible within uncertainties with those submitted for publication by CMS [73], which have smaller statistical uncertainty. In the left panel of Fig. 3, the non-prompt D⁰-meson v_2 is compared with the average v_2 of prompt D⁰, D⁺, and D^{*+} mesons [52]. The non-prompt D⁰-meson v_2 is lower than that of prompt non-strange D mesons with 3.2σ significance in $2 < p_{\text{T}} < 8$ GeV/ c , indicating a different degree of participation to the collective motion of the medium between charm and beauty quarks.

The measured v_2 of non-prompt D⁰ mesons is compared with several theoretical models implementing beauty-quark transport in a hydrodynamically expanding QGP phase [62, 101–107] in the right panel of Fig. 3. All of the considered calculations include collisional interactions between beauty quarks and medium constituents. In addition, the LBT [62, 103], LIDO [101, 107], LGR [104], and Langevin [105,

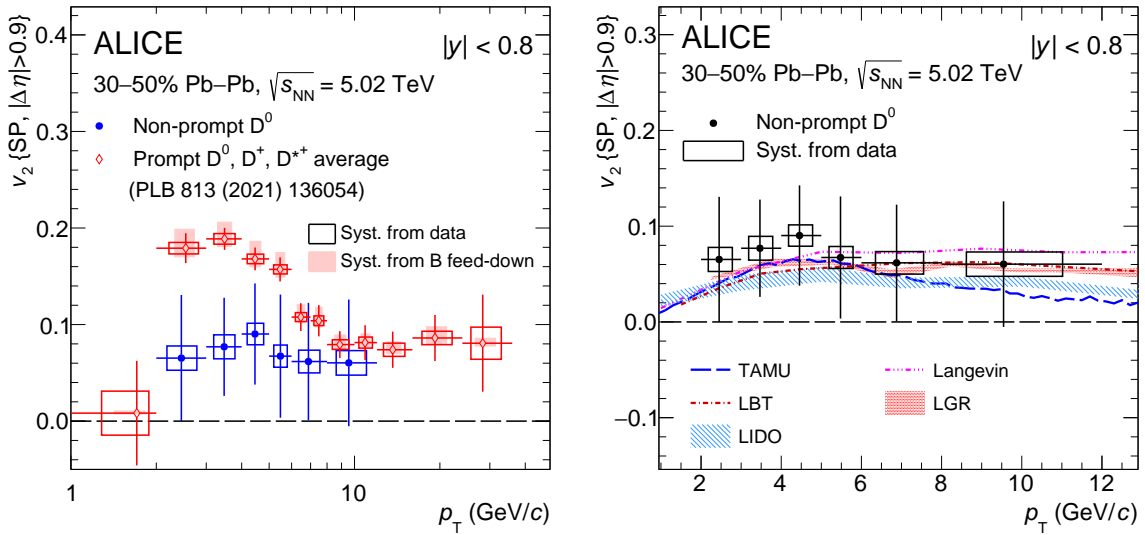


Figure 3: Left panel: Elliptic flow v_2 of non-prompt D^0 mesons (blue points) and average of prompt non-strange D mesons [52] (red points) as a function of p_T in 30–50% Pb–Pb collisions at $\sqrt{s_{\text{NN}}} = 5.02 \text{ TeV}$. The symbols are positioned at the average p_T of the reconstructed D^0 mesons. Statistical uncertainties are shown as vertical lines and systematic uncertainties as boxes. Right panel: non-prompt D^0 -meson v_2 compared with model calculations [62, 101–107].

106] models also include radiative processes. Beauty-quark hadronisation via coalescence is considered for all models in addition to the fragmentation mechanism. Although the models are implemented with different assumptions on the interactions in the QGP and hadronic phases, and on the medium expansion, all of them provide a reasonable description of the measurement within uncertainties. More precise measurements will further constrain model parameters, especially on the spatial diffusion coefficient of beauty quarks, which are implemented differently in the various models.

Figure 4 shows the comparison between the v_2 of electrons from beauty-hadron decays ($b(\rightarrow c) \rightarrow e$) [71] and the non-prompt D^0 -meson v_2 measurements. They are compatible in the common p_T interval within uncertainties. The LIDO model provides reasonable descriptions for these measurements and is consistent with the p_T shape in the data. Note that, the p_T of beauty-decay hadrons is not the same p_T of B mesons due to the decay kinematics. The good agreement between the predictions for B -meson and non-prompt D^0 -meson v_2 from LIDO indicates that the decay kinematics do not play a significant role in the beauty-hadron v_2 measurements.

5 Conclusions

The measurement of the non-prompt D^0 -meson v_2 in midcentral Pb–Pb collisions (30–50% centrality class) at $\sqrt{s_{\text{NN}}} = 5.02 \text{ TeV}$ is presented in the transverse momentum interval $2 < p_T < 12 \text{ GeV}/c$. The non-prompt D^0 -meson v_2 is found to be positive with a significance of 2.7σ and it is lower by 3.2σ than the prompt non-strange D -meson v_2 (average of D^0, D^+ , and D^{*+}) in the range $2 < p_T < 8 \text{ GeV}/c$. The measurement is important for the understanding of the degree of thermalisation of beauty quarks in the QGP. Future data samples to be collected with the upgraded ALICE detector in Run 3 will allow for higher-precision measurements of the non-prompt D^0 -meson v_2 and R_{AA} [108]. These measurements will provide important constraints to model predictions, and allow for accurate extraction of the spatial diffusion coefficient of beauty quarks.

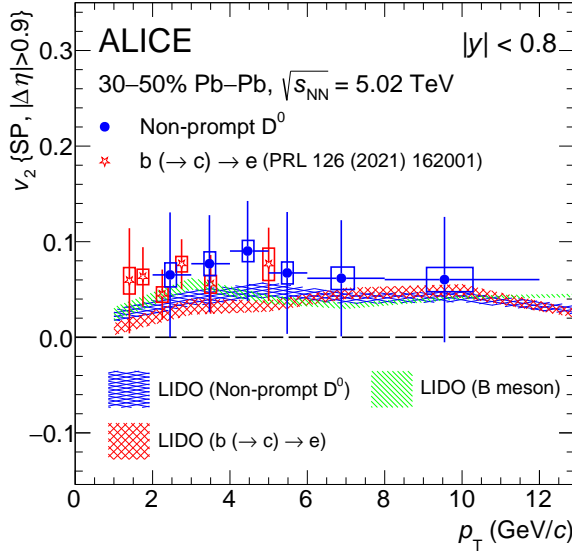


Figure 4: Elliptic flow v_2 of non-prompt D^0 mesons (blue points) and electrons from beauty-hadron decays [71] (red points) as a function of p_T in 30–50% Pb–Pb collisions at $\sqrt{s_{\text{NN}}} = 5.02 \text{ TeV}$, compared with the LIDO model predictions [101, 107].

Acknowledgements

The ALICE Collaboration would like to thank all its engineers and technicians for their invaluable contributions to the construction of the experiment and the CERN accelerator teams for the outstanding performance of the LHC complex. The ALICE Collaboration gratefully acknowledges the resources and support provided by all Grid centres and the Worldwide LHC Computing Grid (WLCG) collaboration. The ALICE Collaboration acknowledges the following funding agencies for their support in building and running the ALICE detector: A. I. Alikhanyan National Science Laboratory (Yerevan Physics Institute) Foundation (ANSL), State Committee of Science and World Federation of Scientists (WFS), Armenia; Austrian Academy of Sciences, Austrian Science Fund (FWF): [M 2467-N36] and Nationalstiftung für Forschung, Technologie und Entwicklung, Austria; Ministry of Communications and High Technologies, National Nuclear Research Center, Azerbaijan; Conselho Nacional de Desenvolvimento Científico e Tecnológico (CNPq), Financiadora de Estudos e Projetos (Finep), Fundação de Amparo à Pesquisa do Estado de São Paulo (FAPESP) and Universidade Federal do Rio Grande do Sul (UFRGS), Brazil; Bulgarian Ministry of Education and Science, within the National Roadmap for Research Infrastructures 2020-2027 (object CERN), Bulgaria; Ministry of Education of China (MOEC), Ministry of Science & Technology of China (MSTC) and National Natural Science Foundation of China (NSFC), China; Ministry of Science and Education and Croatian Science Foundation, Croatia; Centro de Aplicaciones Tecnológicas y Desarrollo Nuclear (CEADEN), Cubaenergía, Cuba; Ministry of Education, Youth and Sports of the Czech Republic, Czech Republic; The Danish Council for Independent Research | Natural Sciences, the VILLUM FONDEN and Danish National Research Foundation (DNRF), Denmark; Helsinki Institute of Physics (HIP), Finland; Commissariat à l’Energie Atomique (CEA) and Institut National de Physique Nucléaire et de Physique des Particules (IN2P3) and Centre National de la Recherche Scientifique (CNRS), France; Bundesministerium für Bildung und Forschung (BMBF) and GSI Helmholtzzentrum für Schwerionenforschung GmbH, Germany; General Secretariat for Research and Technology, Ministry of Education, Research and Religions, Greece; National Research, Development and Innovation Office, Hungary; Department of Atomic Energy Government of India (DAE), Department of Science and Technology, Government of India (DST), University Grants Commission, Government of India (UGC) and Council of Scientific and Industrial Research (CSIR), India; National

Research and Innovation Agency - BRIN, Indonesia; Istituto Nazionale di Fisica Nucleare (INFN), Italy; Japanese Ministry of Education, Culture, Sports, Science and Technology (MEXT) and Japan Society for the Promotion of Science (JSPS) KAKENHI, Japan; Consejo Nacional de Ciencia (CONACYT) y Tecnología, through Fondo de Cooperación Internacional en Ciencia y Tecnología (FONCICYT) and Dirección General de Asuntos del Personal Académico (DGAPA), Mexico; Nederlandse Organisatie voor Wetenschappelijk Onderzoek (NWO), Netherlands; The Research Council of Norway, Norway; Commission on Science and Technology for Sustainable Development in the South (COMSATS), Pakistan; Pontificia Universidad Católica del Perú, Peru; Ministry of Education and Science, National Science Centre and WUT ID-UB, Poland; Korea Institute of Science and Technology Information and National Research Foundation of Korea (NRF), Republic of Korea; Ministry of Education and Scientific Research, Institute of Atomic Physics, Ministry of Research and Innovation and Institute of Atomic Physics and University Politehnica of Bucharest, Romania; Ministry of Education, Science, Research and Sport of the Slovak Republic, Slovakia; National Research Foundation of South Africa, South Africa; Swedish Research Council (VR) and Knut & Alice Wallenberg Foundation (KAW), Sweden; European Organization for Nuclear Research, Switzerland; Suranaree University of Technology (SUT), National Science and Technology Development Agency (NSTDA), Thailand Science Research and Innovation (TSRI) and National Science, Research and Innovation Fund (NSRF), Thailand; Turkish Energy, Nuclear and Mineral Research Agency (TENMAK), Turkey; National Academy of Sciences of Ukraine, Ukraine; Science and Technology Facilities Council (STFC), United Kingdom; National Science Foundation of the United States of America (NSF) and United States Department of Energy, Office of Nuclear Physics (DOE NP), United States of America. In addition, individual groups or members have received support from: European Research Council, Strong 2020 - Horizon 2020 (grant nos. 950692, 824093), European Union; Academy of Finland (Center of Excellence in Quark Matter) (grant nos. 346327, 346328), Finland.

References

- [1] **NA50** Collaboration, M. C. Abreu *et al.*, “Evidence for deconfinement of quarks and gluons from the J/ ψ suppression pattern measured in Pb–Pb collisions at the CERN-SPS”, *Phys. Lett. B* **477** (2000) 28–36.
- [2] **WA97** Collaboration, E. Andersen *et al.*, “Strangeness enhancement at mid-rapidity in Pb–Pb collisions at 158 A GeV/c”, *Phys. Lett. B* **449** (1999) 401–406.
- [3] **BRAHMS** Collaboration, I. Arsene *et al.*, “Quark gluon plasma and color glass condensate at RHIC? The Perspective from the BRAHMS experiment”, *Nucl. Phys. A* **757** (2005) 1–27, arXiv:nucl-ex/0410020 [nucl-ex].
- [4] **PHENIX** Collaboration, K. Adcox *et al.*, “Formation of dense partonic matter in relativistic nucleus–nucleus collisions at RHIC: Experimental evaluation by the PHENIX collaboration”, *Nucl. Phys. A* **757** (2005) 184–283, arXiv:nucl-ex/0410003 [nucl-ex].
- [5] **PHOBOS** Collaboration, B. B. Back *et al.*, “The PHOBOS perspective on discoveries at RHIC”, *Nucl. Phys. A* **757** (2005) 28–101, arXiv:nucl-ex/0410022 [nucl-ex].
- [6] **STAR** Collaboration, J. Adams *et al.*, “Experimental and theoretical challenges in the search for the quark–gluon plasma: The STAR Collaboration’s critical assessment of the evidence from RHIC collisions”, *Nucl. Phys. A* **757** (2005) 102–183, arXiv:nucl-ex/0501009 [nucl-ex].
- [7] G. Roland, K. Safarik, and P. Steinberg, “Heavy-ion collisions at the LHC”, *Prog. Part. Nucl. Phys.* **77** (2014) 70–127.

- [8] P. Braun-Munzinger, V. Koch, T. Schäfer, and J. Stachel, “Properties of hot and dense matter from relativistic heavy ion collisions”, *Phys. Rept.* **621** (2016) 76–126, arXiv:1510.00442 [nucl-th].
- [9] **ALICE** Collaboration, “The ALICE experiment – A journey through QCD”, arXiv:2211.04384 [nucl-ex].
- [10] U. Heinz and R. Snellings, “Collective flow and viscosity in relativistic heavy-ion collisions”, *Ann. Rev. Nucl. Part. Sci.* **63** (2013) 123–151, arXiv:1301.2826 [nucl-th].
- [11] F.-M. Liu and S.-X. Liu, “Quark-gluon plasma formation time and direct photons from heavy ion collisions”, *Phys. Rev. C* **89** (2014) 034906, arXiv:1212.6587 [nucl-th].
- [12] A. Andronic *et al.*, “Heavy-flavour and quarkonium production in the LHC era: from proton–proton to heavy-ion collisions”, *Eur. Phys. J. C* **76** (2016) 107, arXiv:1506.03981 [nucl-ex].
- [13] E. Braaten and M. H. Thoma, “Energy loss of a heavy quark in the quark–gluon plasma”, *Phys. Rev. D* **44** (1991) R2625.
- [14] **PHENIX** Collaboration, A. Adare *et al.*, “Heavy Quark Production in $p + p$ and Energy Loss and Flow of Heavy Quarks in Au+Au Collisions at $\sqrt{s_{\text{NN}}} = 200 \text{ GeV}$ ”, *Phys. Rev. C* **84** (2011) 044905, arXiv:1005.1627 [nucl-ex].
- [15] **STAR** Collaboration, B. Abelev *et al.*, “Transverse momentum and centrality dependence of high- p_T non-photonic electron suppression in Au+Au collisions at $\sqrt{s_{\text{NN}}} = 200 \text{ GeV}$ ”, *Phys. Rev. Lett.* **98** (2007) 192301, arXiv:nucl-ex/0607012 [nucl-ex]. [Erratum: *Phys. Rev. Lett.* **106** (2011) 159902].
- [16] **STAR** Collaboration, L. Adamczyk *et al.*, “Observation of D⁰ Meson Nuclear Modifications in Au+Au Collisions at $\sqrt{s_{\text{NN}}} = 200 \text{ GeV}$ ”, *Phys. Rev. Lett.* **113** (2014) 142301, arXiv:1404.6185 [nucl-ex]. [Erratum: *Phys. Rev. Lett.* **121** (2018) 229901].
- [17] **PHENIX** Collaboration, S. S. Adler *et al.*, “Nuclear modification of electron spectra and implications for heavy quark energy loss in Au+Au collisions at $\sqrt{s_{\text{NN}}} = 200 \text{ GeV}$ ”, *Phys. Rev. Lett.* **96** (2006) 032301, arXiv:nucl-ex/0510047 [nucl-ex].
- [18] **PHENIX** Collaboration, A. Adare *et al.*, “Single electron yields from semileptonic charm and bottom hadron decays in Au+Au collisions at $\sqrt{s_{\text{NN}}} = 200 \text{ GeV}$ ”, *Phys. Rev. C* **93** (2016) 034904, arXiv:1509.04662 [nucl-ex].
- [19] **ALICE** Collaboration, J. Adam *et al.*, “Transverse momentum dependence of D-meson production in Pb–Pb collisions at $\sqrt{s_{\text{NN}}} = 2.76 \text{ TeV}$ ”, *JHEP* **03** (2016) 081, arXiv:1509.06888 [nucl-ex].
- [20] **ALICE** Collaboration, B. Abelev *et al.*, “Production of muons from heavy flavour decays at forward rapidity in pp and Pb–Pb collisions at $\sqrt{s_{\text{NN}}} = 2.76 \text{ TeV}$ ”, *Phys. Rev. Lett.* **109** (2012) 112301, arXiv:1205.6443 [hep-ex].
- [21] **ALICE** Collaboration, J. Adam *et al.*, “Measurement of the production of high- p_T electrons from heavy-flavour hadron decays in Pb–Pb collisions at $\sqrt{s_{\text{NN}}} = 2.76 \text{ TeV}$ ”, *Phys. Lett. B* **771** (2017) 467–481, arXiv:1609.07104 [nucl-ex].
- [22] **ALICE** Collaboration, J. Adam *et al.*, “Measurement of electrons from beauty-hadron decays in p–Pb collisions at $\sqrt{s_{\text{NN}}} = 5.02 \text{ TeV}$ and Pb–Pb collisions at $\sqrt{s_{\text{NN}}} = 2.76 \text{ TeV}$ ”, *JHEP* **07** (2017) 052, arXiv:1609.03898 [nucl-ex].

- [23] CMS Collaboration, V. Khachatryan *et al.*, “Suppression and azimuthal anisotropy of prompt and nonprompt J/ ψ production in PbPb collisions at $\sqrt{s_{\text{NN}}} = 2.76 \text{ TeV}$ ”, *Eur. Phys. J. C* **77** (2017) 252, arXiv:1610.00613 [nucl-ex].
- [24] CMS Collaboration, A. M. Sirunyan *et al.*, “Nuclear modification factor of D⁰ mesons in PbPb collisions at $\sqrt{s_{\text{NN}}} = 5.02 \text{ TeV}$ ”, *Phys. Lett. B* **782** (2018) 474–496, arXiv:1708.04962 [nucl-ex].
- [25] ALICE Collaboration, S. Acharya *et al.*, “Measurement of D⁰, D⁺, D^{*+} and D_s⁺ production in Pb–Pb collisions at $\sqrt{s_{\text{NN}}} = 5.02 \text{ TeV}$ ”, *JHEP* **10** (2018) 174, arXiv:1804.09083 [nucl-ex].
- [26] CMS Collaboration, A. M. Sirunyan *et al.*, “Measurement of B_s⁰ meson production in pp and PbPb collisions at $\sqrt{s_{\text{NN}}} = 5.02 \text{ TeV}$ ”, *Phys. Lett. B* **796** (2019) 168–190, arXiv:1810.03022 [hep-ex].
- [27] CMS Collaboration, A. M. Sirunyan *et al.*, “Measurement of the B $^\pm$ Meson Nuclear Modification Factor in Pb-Pb Collisions at $\sqrt{s_{\text{NN}}} = 5.02 \text{ TeV}$ ”, *Phys. Rev. Lett.* **119** (2017) 152301, arXiv:1705.04727 [hep-ex].
- [28] ALICE Collaboration, S. Acharya *et al.*, “Prompt D⁰, D⁺, and D^{*+} production in Pb–Pb collisions at $\sqrt{s_{\text{NN}}} = 5.02 \text{ TeV}$ ”, *JHEP* **01** (2022) 174, arXiv:2110.09420 [nucl-ex].
- [29] ALICE Collaboration, S. Acharya *et al.*, “Measurement of prompt D_s⁺-meson production and azimuthal anisotropy in Pb–Pb collisions at $\sqrt{s_{\text{NN}}} = 5.02 \text{ TeV}$ ”, *Phys. Lett. B* **827** (2022) 136986, arXiv:2110.10006 [nucl-ex].
- [30] ALICE Collaboration, S. Acharya *et al.*, “Constraining hadronization mechanisms with Λ_c^+ / D^0 production ratios in Pb–Pb collisions at $\sqrt{s_{\text{NN}}} = 5.02 \text{ TeV}$ ”, *Phys. Lett. B* **839** (2023) 137796, arXiv:2112.08156 [nucl-ex].
- [31] ALICE Collaboration, S. Acharya *et al.*, “Measurement of beauty production via non-prompt D⁰ mesons in Pb–Pb collisions at $\sqrt{s_{\text{NN}}} = 5.02 \text{ TeV}$ ”, *JHEP* **12** (2022) 126, arXiv:2202.00815 [nucl-ex].
- [32] ALICE Collaboration, S. Acharya *et al.*, “Measurement of beauty-strange meson production in Pb–Pb collisions at sNN=5.02TeV via non-prompt Ds+ mesons”, *Phys. Lett. B* **846** (2023) 137561, arXiv:2204.10386 [nucl-ex].
- [33] ALICE Collaboration, S. Acharya *et al.*, “Measurement of electrons from beauty-hadron decays in pp and Pb–Pb collisions at sNN=5.02 TeV”, *Phys. Rev. C* **108** (2023) 034906, arXiv:2211.13985 [nucl-ex].
- [34] J.-Y. Ollitrault, “Anisotropy as a signature of transverse collective flow”, *Phys. Rev. D* **46** (1992) 229–245.
- [35] S. Voloshin and Y. Zhang, “Flow study in relativistic nuclear collisions by Fourier expansion of Azimuthal particle distributions”, *Z. Phys. C* **70** (1996) 665–672, arXiv:hep-ph/9407282 [hep-ph].
- [36] S. Batsouli, S. Kelly, M. Gyulassy, and J. L. Nagle, “Does the charm flow at RHIC?”, *Phys. Lett. B* **557** (2003) 26–32, arXiv:nucl-th/0212068 [nucl-th].
- [37] D. Molnar, “Charm elliptic flow from quark coalescence dynamics”, *J. Phys. G* **31** (2005) S421–S428, arXiv:nucl-th/0410041 [nucl-th].

- [38] V. Greco, C. M. Ko, and R. Rapp, “Quark coalescence for charmed mesons in ultrarelativistic heavy ion collisions”, *Phys. Lett. B* **595** (2004) 202–208, arXiv:nucl-th/0312100 [nucl-th].
- [39] M. Gyulassy, I. Vitev, and X. N. Wang, “High p_{T} azimuthal asymmetry in noncentral A+A at RHIC”, *Phys. Rev. Lett.* **86** (2001) 2537–2540, arXiv:nucl-th/0012092 [nucl-th].
- [40] E. V. Shuryak, “The Azimuthal asymmetry at large p_{T} seem to be too large for a ‘jet quenching’”, *Phys. Rev. C* **66** (2002) 027902, arXiv:nucl-th/0112042 [nucl-th].
- [41] **PHENIX** Collaboration, A. Adare *et al.*, “Energy Loss and Flow of Heavy Quarks in Au+Au Collisions at $\sqrt{s_{\text{NN}}} = 200 \text{ GeV}$ ”, *Phys. Rev. Lett.* **98** (2007) 172301, arXiv:nucl-ex/0611018 [nucl-ex].
- [42] **STAR** Collaboration, L. Adamczyk *et al.*, “Elliptic flow of electrons from heavy-flavor hadron decays in Au+Au collisions at $\sqrt{s_{\text{NN}}} = 200, 62.4, \text{ and } 39 \text{ GeV}$ ”, *Phys. Rev. C* **95** (2017) 034907, arXiv:1405.6348 [hep-ex].
- [43] **STAR** Collaboration, L. Adamczyk *et al.*, “Measurement of D⁰ Azimuthal Anisotropy at Midrapidity in Au+Au Collisions at $\sqrt{s_{\text{NN}}} = 200 \text{ GeV}$ ”, *Phys. Rev. Lett.* **118** (2017) 212301, arXiv:1701.06060 [nucl-ex].
- [44] **ALICE** Collaboration, B. Abelev *et al.*, “D meson elliptic flow in non-central Pb–Pb collisions at $\sqrt{s_{\text{NN}}} = 2.76 \text{ TeV}$ ”, *Phys. Rev. Lett.* **111** (2013) 102301, arXiv:1305.2707 [nucl-ex].
- [45] **ALICE** Collaboration, B. Abelev *et al.*, “Azimuthal anisotropy of D meson production in Pb–Pb collisions at $\sqrt{s_{\text{NN}}} = 2.76 \text{ TeV}$ ”, *Phys. Rev. C* **90** (2014) 034904, arXiv:1405.2001 [nucl-ex].
- [46] **ALICE** Collaboration, J. Adam *et al.*, “Elliptic flow of electrons from heavy-flavour hadron decays at mid-rapidity in Pb–Pb collisions at $\sqrt{s_{\text{NN}}} = 2.76 \text{ TeV}$ ”, *JHEP* **09** (2016) 028, arXiv:1606.00321 [nucl-ex].
- [47] **ALICE** Collaboration, J. Adam *et al.*, “Elliptic flow of muons from heavy-flavour hadron decays at forward rapidity in Pb–Pb collisions at $\sqrt{s_{\text{NN}}} = 2.76 \text{ TeV}$ ”, *Phys. Lett. B* **753** (2016) 41–56, arXiv:1507.03134 [nucl-ex].
- [48] **ALICE** Collaboration, S. Acharya *et al.*, “D-meson azimuthal anisotropy in midcentral Pb–Pb collisions at $\sqrt{s_{\text{NN}}} = 5.02 \text{ TeV}$ ”, *Phys. Rev. Lett.* **120** (2018) 102301, arXiv:1707.01005 [nucl-ex].
- [49] **CMS** Collaboration, A. M. Sirunyan *et al.*, “Measurement of prompt D^0 meson azimuthal anisotropy in Pb–Pb collisions at $\sqrt{s_{\text{NN}}} = 5.02 \text{ TeV}$ ”, *Phys. Rev. Lett.* **120** (2018) 202301, arXiv:1708.03497 [nucl-ex].
- [50] **ALICE** Collaboration, S. Acharya *et al.*, “Event-shape engineering for the D-meson elliptic flow in mid-central Pb–Pb collisions at $\sqrt{s_{\text{NN}}} = 5.02 \text{ TeV}$ ”, *JHEP* **02** (2019) 150, arXiv:1809.09371 [nucl-ex].
- [51] **CMS** Collaboration, A. M. Sirunyan *et al.*, “Measurement of prompt D^0 meson azimuthal anisotropy in Pb–Pb collisions at $\sqrt{s_{\text{NN}}} = 5.02 \text{ TeV}$ ”, *Phys. Rev. Lett.* **120** (2018) 202301, arXiv:1708.03497 [nucl-ex].
- [52] **ALICE** Collaboration, S. Acharya *et al.*, “Transverse-momentum and event-shape dependence of D-meson flow harmonics in Pb–Pb collisions at $\sqrt{s_{\text{NN}}} = 5.02 \text{ TeV}$ ”, *Phys. Lett. B* **813** (2021) 136054, arXiv:2005.11131 [nucl-ex].

- [53] CMS Collaboration, A. M. Sirunyan *et al.*, “Measurement of prompt D⁰ and \bar{D}^0 meson azimuthal anisotropy and search for strong electric fields in PbPb collisions at $\sqrt{s_{\text{NN}}} = 5.02 \text{ TeV}$ ”, *Phys. Lett. B* **816** (2021) 136253, arXiv:2009.12628 [hep-ex].
- [54] J. Uphoff, O. Fochler, Z. Xu, and C. Greiner, “Open Heavy Flavor in Pb+Pb Collisions at $\sqrt{s} = 2.76 \text{ TeV}$ within a Transport Model”, *Phys. Lett. B* **717** (2012) 430–435, arXiv:1205.4945 [hep-ph].
- [55] M. He, R. J. Fries, and R. Rapp, “Heavy Flavor at the Large Hadron Collider in a Strong Coupling Approach”, *Phys. Lett. B* **735** (2014) 445–450, arXiv:1401.3817 [nucl-th].
- [56] M. Monteno, W. M. Alberico, A. Beraudo, A. De Pace, A. Molinari, M. Nardi, and F. Prino, “Heavy-flavor dynamics in nucleus-nucleus collisions: from RHIC to LHC”, *J. Phys. G* **38** (2011) 124144, arXiv:1107.0256 [hep-ph].
- [57] S. Cao, G.-Y. Qin, and S. A. Bass, “Heavy-quark dynamics and hadronization in ultrarelativistic heavy-ion collisions: Collisional versus radiative energy loss”, *Phys. Rev. C* **88** (2013) 044907, arXiv:1308.0617 [nucl-th].
- [58] T. Song, H. Berrehrah, D. Cabrera, W. Cassing, and E. Bratkovskaya, “Charm production in Pb + Pb collisions at energies available at the CERN Large Hadron Collider”, *Phys. Rev. C* **93** (2016) 034906, arXiv:1512.00891 [nucl-th].
- [59] M. Nahrgang, J. Aichelin, P. B. Gossiaux, and K. Werner, “Influence of hadronic bound states above T_c on heavy-quark observables in Pb + Pb collisions at the CERN Large Hadron Collider”, *Phys. Rev. C* **89** (2014) 014905, arXiv:1305.6544 [hep-ph].
- [60] J. Uphoff, O. Fochler, Z. Xu, and C. Greiner, “Elastic and radiative heavy quark interactions in ultra-relativistic heavy-ion collisions”, *J. Phys. G* **42** (2015) 115106, arXiv:1408.2964 [hep-ph].
- [61] A. Beraudo, A. De Pace, M. Monteno, M. Nardi, and F. Prino, “Heavy flavors in heavy-ion collisions: quenching, flow and correlations”, *Eur. Phys. J. C* **75** (2015) 121, arXiv:1410.6082 [hep-ph].
- [62] S. Cao, T. Luo, G.-Y. Qin, and X.-N. Wang, “Heavy and light flavor jet quenching at RHIC and LHC energies”, *Phys. Lett. B* **777** (2018) 255–259, arXiv:1703.00822 [nucl-th].
- [63] A. Beraudo, A. De Pace, M. Monteno, M. Nardi, and F. Prino, “Rapidity dependence of heavy-flavour production in heavy-ion collisions within a full 3+1 transport approach: quenching, elliptic and directed flow”, *JHEP* **05** (2021) 279, arXiv:2102.08064 [hep-ph].
- [64] G. D. Moore and D. Teaney, “How much do heavy quarks thermalize in a heavy ion collision?”, *Phys. Rev. C* **71** (2005) 064904, arXiv:hep-ph/0412346 [hep-ph].
- [65] A. Francis, O. Kaczmarek, M. Laine, T. Neuhaus, and H. Ohno, “Nonperturbative estimate of the heavy quark momentum diffusion coefficient”, *Phys. Rev. D* **92** (2015) 116003, arXiv:1508.04543 [hep-lat].
- [66] S. Y. F. Liu and R. Rapp, “Spectral and transport properties of quark-gluon plasma in a nonperturbative approach”, *Eur. Phys. J. A* **56** (2020) 44, arXiv:1612.09138 [nucl-th].
- [67] F. Riek and R. Rapp, “Quarkonia and Heavy-Quark Relaxation Times in the Quark-Gluon Plasma”, *Phys. Rev. C* **82** (2010) 035201, arXiv:1005.0769 [hep-ph].

- [68] F. Capellino, A. Beraudo, A. Dubla, S. Floerchinger, S. Masciocchi, J. Pawłowski, and I. Selyuzhenkov, “Fluid-dynamic approach to heavy-quark diffusion in the quark-gluon plasma”, *Phys. Rev. D* **106** (2022) 034021, arXiv:2205.07692 [nucl-th].
- [69] CMS Collaboration, V. Khachatryan *et al.*, “Suppression and azimuthal anisotropy of prompt and nonprompt J/ ψ production in PbPb collisions at $\sqrt{s_{\text{NN}}} = 2.76$ TeV”, *Eur. Phys. J. C* **77** (2017) 252, arXiv:1610.00613 [nucl-ex].
- [70] ATLAS Collaboration, M. Aaboud *et al.*, “Prompt and non-prompt J/ ψ elliptic flow in Pb+Pb collisions at $\sqrt{s_{\text{NN}}} = 5.02$ TeV with the ATLAS detector”, *Eur. Phys. J. C* **78** (2018) 784, arXiv:1807.05198 [nucl-ex].
- [71] ALICE Collaboration, S. Acharya *et al.*, “Elliptic Flow of Electrons from Beauty-Hadron Decays in Pb–Pb Collisions at $\sqrt{s_{\text{NN}}} = 5.02$ TeV”, *Phys. Rev. Lett.* **126** (2021) 162001, arXiv:2005.11130 [nucl-ex].
- [72] ATLAS Collaboration, G. Aad *et al.*, “Measurement of azimuthal anisotropy of muons from charm and bottom hadrons in Pb+Pb collisions at $\sqrt{s_{\text{NN}}} = 5.02$ TeV with the ATLAS detector”, *Phys. Lett. B* **807** (2020) 135595, arXiv:2003.03565 [nucl-ex].
- [73] CMS Collaboration, “Measurements of azimuthal anisotropy of nonprompt D⁰ mesons in PbPb collisions at $\sqrt{s_{\text{NN}}} = 5.02$ TeV”, arXiv:2212.01636 [nucl-ex].
- [74] M. Luzum and J.-Y. Ollitrault, “Eliminating experimental bias in anisotropic-flow measurements of high-energy nuclear collisions”, *Phys. Rev. C* **87** (2013) 044907, arXiv:1209.2323 [nucl-ex].
- [75] S. A. Voloshin, A. M. Poskanzer, and R. Snellings, “Collective phenomena in non-central nuclear collisions”, *Landolt-Bornstein* **23** (2010) 293–333, arXiv:0809.2949 [nucl-ex].
- [76] ALICE Collaboration, B. Abelev *et al.*, “Performance of the ALICE Experiment at the CERN LHC”, *Int. J. Mod. Phys. A* **29** (2014) 1430044, arXiv:1402.4476 [nucl-ex].
- [77] ALICE Collaboration, K. Aamodt *et al.*, “The ALICE experiment at the CERN LHC”, *JINST* **3** (2008) S08002.
- [78] ALICE Collaboration, K. Aamodt *et al.*, “Alignment of the ALICE Inner Tracking System with cosmic-ray tracks”, *JINST* **5** (2010) P03003, arXiv:1001.0502 [physics.ins-det].
- [79] J. Alme *et al.*, “The ALICE TPC, a large 3-dimensional tracking device with fast readout for ultra-high multiplicity events”, *Nucl. Instrum. Meth. A* **622** (2010) 316–367, arXiv:1001.1950 [physics.ins-det].
- [80] A. Akindinov *et al.*, “Performance of the ALICE Time-Of-Flight detector at the LHC”, *Eur. Phys. J. Plus* **128** (2013) 44.
- [81] ALICE Collaboration, E. Abbas *et al.*, “Performance of the ALICE VZERO system”, *JINST* **8** (2013) P10016, arXiv:1306.3130 [nucl-ex].
- [82] R. Arnaldi *et al.*, “The Zero Degree Calorimeters for the ALICE experiment”, *Nucl. Instrum. Meth. A* **581** (2007) 397–401. [Erratum: *Nucl. Instrum. Meth.A* **604** (2009) 765].
- [83] ALICE Collaboration, J. Adam *et al.*, “Centrality dependence of the charged-particle multiplicity density at midrapidity in Pb–Pb collisions at $\sqrt{s_{\text{NN}}} = 5.02$ TeV”, *Phys. Rev. Lett.* **116** (2016) 222302, arXiv:1512.06104 [nucl-ex].

- [84] **ALICE** Collaboration, “Centrality determination in heavy ion collisions”, Tech. Rep. ALICE-PUBLIC-2018-011, Aug, 2018. <http://cds.cern.ch/record/2636623>.
- [85] **Particle Data Group** Collaboration, R. L. Workman *et al.*, “Review of Particle Physics”, *PTEP* **2022** (2022) 083C01.
- [86] T. Chen and C. Guestrin, “XGBoost: A scalable tree boosting system”, *Proceedings of the 22nd ACM SIGKDD International Conference on Knowledge Discovery and Data Mining* (2016) 785–794, arXiv:1603.02754 [cs.LG].
- [87] X.-N. Wang and M. Gyulassy, “HIJING: A Monte Carlo model for multiple jet production in pp, pA and AA collisions”, *Phys. Rev. D* **44** (1991) 3501–3516.
- [88] T. Sjöstrand, S. Mrenna, and P. Z. Skands, “PYTHIA 6.4 Physics and Manual”, *JHEP* **05** (2006) 026, arXiv:hep-ph/0603175 [hep-ph].
- [89] T. Sjöstrand *et al.*, “An Introduction to PYTHIA 8.2”, *Comput. Phys. Commun.* **191** (2015) 159–177, arXiv:1410.3012 [hep-ph].
- [90] P. Skands, S. Carrazza, and J. Rojo, “Tuning PYTHIA 8.1: the Monash 2013 Tune”, *Eur. Phys. J. C* **74** (2014) 3024, arXiv:1404.5630 [hep-ph].
- [91] R. Brun, F. Carminati, and S. Giani, “CERN Program Library Long Write-up, W5013 GEANT Detector Description and Simulation Tool”, Tech. Rep. CERN-W-5013, 1994. <https://cds.cern.ch/record/1082634>.
- [92] **ALICE** Collaboration, S. Acharya *et al.*, “Measurement of beauty and charm production in pp collisions at $\sqrt{s} = 5.02 \text{ TeV}$ via non-prompt and prompt D mesons”, *JHEP* **05** (2021) 220, arXiv:2102.13601 [nucl-ex].
- [93] **STAR** Collaboration, C. Adler *et al.*, “Elliptic flow from two and four particle correlations in Au+Au collisions at $\sqrt{s_{\text{NN}}} = 130 \text{ GeV}$ ”, *Phys. Rev. C* **66** (2002) 034904, arXiv:nucl-ex/0206001 [nucl-ex].
- [94] I. Selyuzhenkov and S. Voloshin, “Effects of non-uniform acceptance in anisotropic flow measurement”, *Phys. Rev. C* **77** (2008) 034904, arXiv:0707.4672 [nucl-th].
- [95] **ALICE** Collaboration, S. Acharya *et al.*, “Energy dependence and fluctuations of anisotropic flow in Pb-Pb collisions at $\sqrt{s_{\text{NN}}} = 5.02$ and 2.76 TeV ”, *JHEP* **07** (2018) 103, arXiv:1804.02944 [nucl-ex].
- [96] N. Borghini and J. Y. Ollitrault, “Azimuthally sensitive correlations in nucleus-nucleus collisions”, *Phys. Rev. C* **70** (2004) 064905, arXiv:nucl-th/0407041 [nucl-th].
- [97] **CMS** Collaboration, A. M. Sirunyan *et al.*, “Studies of charm and beauty hadron long-range correlations in pp and pPb collisions at LHC energies”, *Phys. Lett. B* **813** (2021) 136036, arXiv:2009.07065 [hep-ex].
- [98] B. Efron, “Bootstrap Methods: Another Look at the Jackknife”, *Annals Statist.* **7** (1979) 1–26.
- [99] M. Cacciari, S. Frixione, and P. Nason, “The p_T spectrum in heavy flavor photoproduction”, *JHEP* **03** (2001) 006, arXiv:hep-ph/0102134 [hep-ph].
- [100] M. Cacciari, M. Greco, and P. Nason, “The p_T spectrum in heavy flavor hadroproduction”, *JHEP* **05** (1998) 007, arXiv:hep-ph/9803400 [hep-ph].

- [101] W. Ke, Y. Xu, and S. A. Bass, “Linearized Boltzmann-Langevin model for heavy quark transport in hot and dense QCD matter”, *Phys. Rev. C* **98** (2018) 064901, arXiv:1806.08848 [nucl-th].
- [102] M. He and R. Rapp, “Hadronization and Charm-Hadron Ratios in Heavy-Ion Collisions”, *Phys. Rev. Lett.* **124** (2020) 042301, arXiv:1905.09216 [nucl-th].
- [103] S. Cao, T. Luo, G.-Y. Qin, and X.-N. Wang, “Linearized Boltzmann transport model for jet propagation in the quark-gluon plasma: Heavy quark evolution”, *Phys. Rev. C* **94** (2016) 014909, arXiv:1605.06447 [nucl-th].
- [104] S. Li, W. Xiong, and R. Wan, “Relativistic Langevin dynamics: charm versus beauty”, *Eur. Phys. J. C* **80** (2020) 1113, arXiv:2012.02489 [hep-ph].
- [105] S.-Q. Li *et al.*, “Heavy flavor quenching and flow: the roles of initial condition, pre-equilibrium evolution, and in-medium interaction”, *Chin. Phys. C* **44** (2020) 114101, arXiv:2005.03330 [nucl-th].
- [106] S.-Q. Li *et al.*, “Scaling behaviors of heavy flavor meson suppression and flow in different nuclear collision systems at the LHC”, *Eur. Phys. J. C* **81** (2021) 1035, arXiv:2108.06648 [hep-ph].
- [107] W. Ke, Y. Xu, and S. A. Bass, “Modified Boltzmann approach for modeling the splitting vertices induced by the hot QCD medium in the deep Landau-Pomeranchuk-Migdal region”, *Phys. Rev. C* **100** (2019) 064911, arXiv:1810.08177 [nucl-th].
- [108] Z. Citron *et al.*, “Report from Working Group 5: Future physics opportunities for high-density QCD at the LHC with heavy-ion and proton beams”, *CERN Yellow Rep. Monogr.* **7** (2019) 1159–1410, arXiv:1812.06772 [hep-ph].

A The ALICE Collaboration

S. Acharya ¹²⁶, D. Adamová ⁸⁶, G. Aglieri Rinella ³³, M. Agnello ³⁰, N. Agrawal ⁵¹, Z. Ahammed ¹³⁴, S. Ahmad ¹⁶, S.U. Ahn ⁷¹, I. Ahuja ³⁸, A. Akindinov ¹⁴², M. Al-Turany ⁹⁷, D. Aleksandrov ¹⁴², B. Alessandro ⁵⁶, H.M. Alfanda ⁶, R. Alfaro Molina ⁶⁷, B. Ali ¹⁶, A. Alici ²⁶, N. Alizadehvandchali ¹¹⁵, A. Alkin ³³, J. Alme ²¹, G. Alocco ⁵², T. Alt ⁶⁴, A.R. Altamura ⁵⁰, I. Altsybeev ⁹⁵, M.N. Anaam ⁶, C. Andrei ⁴⁶, N. Andreou ¹¹⁴, A. Andronic ¹³⁷, V. Anguelov ⁹⁴, F. Antinori ⁵⁴, P. Antonioli ⁵¹, N. Apadula ⁷⁴, L. Aphecetche ¹⁰³, H. Appelshäuser ⁶⁴, C. Arata ⁷³, S. Arcelli ²⁶, M. Aresti ²³, R. Arnaldi ⁵⁶, J.G.M.C.A. Arneiro ¹¹⁰, I.C. Arsene ²⁰, M. Arslanbekov ¹³⁹, A. Augustinus ³³, R. Averbeck ⁹⁷, M.D. Azmi ¹⁶, H. Baba ¹²³, A. Badalà ⁵³, J. Bae ¹⁰⁴, Y.W. Baek ⁴¹, X. Bai ¹¹⁹, R. Bailhache ⁶⁴, Y. Bailung ⁴⁸, A. Balibino ³⁰, A. Baldissari ¹²⁹, B. Balis ², D. Banerjee ⁴, Z. Banoo ⁹¹, R. Barbera ²⁷, F. Barile ³², L. Barioglio ⁹⁵, M. Barlou ⁷⁸, B. Barman ⁴², G.G. Barnaföldi ¹³⁸, L.S. Barnby ⁸⁵, V. Barret ¹²⁶, L. Barreto ¹¹⁰, C. Bartels ¹¹⁸, K. Barth ³³, E. Bartsch ⁶⁴, N. Bastid ¹²⁶, S. Basu ⁷⁵, G. Batigne ¹⁰³, D. Battistini ⁹⁵, B. Batyunya ¹⁴³, D. Bauri ⁴⁷, J.L. Bazo Alba ¹⁰¹, I.G. Bearden ⁸³, C. Beattie ¹³⁹, P. Becht ⁹⁷, D. Behera ⁴⁸, I. Belikov ¹²⁸, A.D.C. Bell Hechavarria ¹³⁷, F. Bellini ²⁶, R. Bellwied ¹¹⁵, S. Belokurova ¹⁴², Y.A.V. Beltran ⁴⁵, G. Bencedi ¹³⁸, S. Beole ²⁵, Y. Berdnikov ¹⁴², A. Berdnikova ⁹⁴, L. Bergmann ⁹⁴, M.G. Besoiu ⁶³, L. Betev ³³, P.P. Bhaduri ¹³⁴, A. Bhasin ⁹¹, M.A. Bhat ⁴, B. Bhattacharjee ⁴², L. Bianchi ²⁵, N. Bianchi ⁴⁹, J. Bielčík ³⁶, J. Bielčíková ⁸⁶, J. Biernat ¹⁰⁷, A.P. Bigot ¹²⁸, A. Bilandzic ⁹⁵, G. Biro ¹³⁸, S. Biswas ⁴, N. Bize ¹⁰³, J.T. Blair ¹⁰⁸, D. Blau ¹⁴², M.B. Blidaru ⁹⁷, N. Bluhme ³⁹, C. Blume ⁶⁴, G. Boca ^{22,55}, F. Bock ⁸⁷, T. Bodova ²¹, A. Bogdanov ¹⁴², S. Boi ²³, J. Bok ⁵⁸, L. Boldizsár ¹³⁸, M. Bombara ³⁸, P.M. Bond ³³, G. Bonomi ^{133,55}, H. Borel ¹²⁹, A. Borissov ¹⁴², A.G. Borquez Carcamo ⁹⁴, H. Bossi ¹³⁹, E. Botta ²⁵, Y.E.M. Bouziani ⁶⁴, L. Bratrud ⁶⁴, P. Braun-Munzinger ⁹⁷, M. Bregant ¹¹⁰, M. Broz ³⁶, G.E. Bruno ^{96,32}, M.D. Buckland ²⁴, D. Budnikov ¹⁴², H. Buesching ⁶⁴, S. Bufalino ³⁰, P. Buhler ¹⁰², N. Burmasov ¹⁴², Z. Buthelezi ^{68,122}, A. Bylinkin ²¹, S.A. Bysiak ¹⁰⁷, M. Cai ⁶, H. Caines ¹³⁹, A. Caliva ²⁹, E. Calvo Villar ¹⁰¹, J.M.M. Camacho ¹⁰⁹, P. Camerini ²⁴, F.D.M. Canedo ¹¹⁰, M. Carabas ¹²⁵, A.A. Carballo ³³, F. Carnesecchi ³³, R. Caron ¹²⁷, L.A.D. Carvalho ¹¹⁰, J. Castillo Castellanos ¹²⁹, F. Catalano ^{33,25}, C. Ceballos Sanchez ¹⁴³, I. Chakaberia ⁷⁴, P. Chakraborty ⁴⁷, S. Chandra ¹³⁴, S. Chapelard ³³, M. Chartier ¹¹⁸, S. Chattopadhyay ¹³⁴, S. Chattopadhyay ⁹⁹, T.G. Chavez ⁴⁵, T. Cheng ^{97,6}, C. Cheshkov ¹²⁷, B. Cheynis ¹²⁷, V. Chibante Barroso ³³, D.D. Chinellato ¹¹¹, E.S. Chizzali ^{I,95}, J. Cho ⁵⁸, S. Cho ⁵⁸, P. Chochula ³³, D. Choudhury ⁴², P. Christakoglou ⁸⁴, C.H. Christensen ⁸³, P. Christiansen ⁷⁵, T. Chujo ¹²⁴, M. Ciaccio ³⁰, C. Cicalo ⁵², F. Cindolo ⁵¹, M.R. Ciupek ⁹⁷, G. Clai ^{II,51}, F. Colamaria ⁵⁰, J.S. Colburn ¹⁰⁰, D. Colella ^{96,32}, M. Colocci ²⁶, M. Concas ^{III,33}, G. Conesa Balbastre ⁷³, Z. Conesa del Valle ¹³⁰, G. Contin ²⁴, J.G. Contreras ³⁶, M.L. Coquet ¹²⁹, P. Cortese ^{132,56}, M.R. Cosentino ¹¹², F. Costa ³³, S. Costanza ^{22,55}, C. Cot ¹³⁰, J. Crkovská ⁹⁴, P. Crochet ¹²⁶, R. Cruz-Torres ⁷⁴, P. Cui ⁶, A. Dainese ⁵⁴, M.C. Danisch ⁹⁴, A. Danu ⁶³, P. Das ⁸⁰, P. Das ⁴, S. Das ⁴, A.R. Dash ¹³⁷, S. Dash ⁴⁷, R.M.H. David ⁴⁵, A. De Caro ²⁹, G. de Cataldo ⁵⁰, J. de Cuveland ³⁹, A. De Falco ²³, D. De Gruttola ²⁹, N. De Marco ⁵⁶, C. De Martin ²⁴, S. De Pasquale ²⁹, R. Deb ¹³³, R. Del Grande ⁹⁵, L. Dello Stritto ²⁹, W. Deng ⁶, P. Dhankher ¹⁹, D. Di Bari ³², A. Di Mauro ³³, B. Diab ¹²⁹, R.A. Diaz ^{143,7}, T. Dietel ¹¹³, Y. Ding ⁶, J. Ditzel ⁶⁴, R. Divià ³³, D.U. Dixit ¹⁹, Ø. Djuvvslund ²¹, U. Dmitrieva ¹⁴², A. Dobrin ⁶³, B. Döningus ⁶⁴, J.M. Dubinski ¹³⁵, A. Dubla ⁹⁷, S. Dudi ⁹⁰, P. Dupieux ¹²⁶, M. Durkac ¹⁰⁶, N. Dzalaiova ¹³, T.M. Eder ¹³⁷, R.J. Ehlers ⁷⁴, F. Eisenhut ⁶⁴, R. Ejima ⁹², D. Elia ⁵⁰, B. Erasmus ¹⁰³, F. Ercolelli ²⁶, F. Erhardt ⁸⁹, M.R. Ersdal ²¹, B. Espagnon ¹³⁰, G. Eulisse ³³, D. Evans ¹⁰⁰, S. Evdokimov ¹⁴², L. Fabbietti ⁹⁵, M. Faggion ²⁸, J. Faivre ⁷³, F. Fan ⁶, W. Fan ⁷⁴, A. Fantoni ⁴⁹, M. Fasel ⁸⁷, P. Fecchio ³⁰, A. Feliciello ⁵⁶, G. Feofilov ¹⁴², A. Fernández Téllez ⁴⁵, L. Ferrandi ¹¹⁰, M.B. Ferrer ³³, A. Ferrero ¹²⁹, C. Ferrero ⁵⁶, A. Ferretti ²⁵, V.J.G. Feuillard ⁹⁴, V. Filova ³⁶, D. Finogeev ¹⁴², F.M. Fionda ⁵², F. Flor ¹¹⁵, A.N. Flores ¹⁰⁸, S. Foertsch ⁶⁸, I. Fokin ⁹⁴, S. Fokin ¹⁴², E. Fragiocomo ⁵⁷, E. Frajna ¹³⁸, U. Fuchs ³³, N. Funicello ²⁹, C. Forget ⁷³, A. Furs ¹⁴², T. Fusayasu ⁹⁸, J.J. Gaardhøje ⁸³, M. Gagliardi ²⁵, A.M. Gago ¹⁰¹, T. Gahlaut ⁴⁷, C.D. Galvan ¹⁰⁹, D.R. Gangadharan ¹¹⁵, P. Ganoti ⁷⁸, C. Garabatos ⁹⁷, A.T. Garcia ¹³⁰, J.R.A. Garcia ⁴⁵, E. Garcia-Solis ⁹, C. Gargiulo ³³, P. Gasik ⁹⁷, A. Gautam ¹¹⁷, M.B. Gay Ducati ⁶⁶, M. Germain ¹⁰³, A. Ghimouz ¹²⁴, C. Ghosh ¹³⁴, M. Giacalone ⁵¹, G. Gioachin ³⁰, P. Giubellino ^{97,56}, P. Giubilato ²⁸, A.M.C. Glaenzer ¹²⁹, P. Glässel ⁹⁴, E. Glimos ¹²¹, D.J.Q. Goh ⁷⁶, V. Gonzalez ¹³⁶, M. Gorgon ², K. Goswami ⁴⁸, S. Gotovac ³⁴, V. Grabski ⁶⁷, L.K. Graczykowski ¹³⁵, E. Grecka ⁸⁶, A. Grelli ⁵⁹, C. Grigoras ³³, V. Grigoriev ¹⁴², S. Grigoryan ^{143,1}, F. Grossa ³³, J.F. Grosse-Oetringhaus ³³, R. Grosso ⁹⁷, D. Grund ³⁶, N.A. Grunwald ⁹⁴, G.G. Guardiano ¹¹¹, R. Guernane ⁷³, M. Guilbaud ¹⁰³,

- K. Gulbrandsen ⁶⁴, T. Gundem ⁶⁴, T. Gunji ¹²³, W. Guo ⁶, A. Gupta ⁹¹, R. Gupta ⁹¹, R. Gupta ⁴⁸, S.P. Guzman ⁴⁵, K. Gwizdziel ¹³⁵, L. Gyulai ¹³⁸, C. Hadjidakis ¹³⁰, F.U. Haider ⁹¹, S. Haidlova ³⁶, H. Hamagaki ⁷⁶, A. Hamdi ⁷⁴, Y. Han ¹⁴⁰, B.G. Hanley ¹³⁶, R. Hannigan ¹⁰⁸, J. Hansen ⁷⁵, M.R. Haque ¹³⁵, J.W. Harris ¹³⁹, A. Harton ⁹, H. Hassan ¹¹⁶, D. Hatzifotiadou ⁵¹, P. Hauer ⁴³, L.B. Havener ¹³⁹, S.T. Heckel ⁹⁵, E. Hellbär ⁹⁷, H. Helstrup ³⁵, M. Hemmer ⁶⁴, T. Herman ³⁶, G. Herrera Corral ⁸, F. Herrmann ¹³⁷, S. Herrmann ¹²⁷, K.F. Hetland ³⁵, B. Heybeck ⁶⁴, H. Hillemanns ³³, B. Hippolyte ¹²⁸, F.W. Hoffmann ⁷⁰, B. Hofman ⁵⁹, G.H. Hong ¹⁴⁰, M. Horst ⁹⁵, A. Horzyk ², Y. Hou ⁶, P. Hristov ³³, C. Hughes ¹²¹, P. Huhn ⁶⁴, L.M. Huhta ¹¹⁶, T.J. Humanic ⁸⁸, A. Hutson ¹¹⁵, D. Hutter ³⁹, R. Ilkaev ¹⁴², H. Ilyas ¹⁴, M. Inaba ¹²⁴, G.M. Innocenti ³³, M. Ippolitov ¹⁴², A. Isakov ^{84,86}, T. Isidori ¹¹⁷, M.S. Islam ⁹⁹, M. Ivanov ¹³, M. Ivanov ⁹⁷, V. Ivanov ¹⁴², K.E. Iversen ⁷⁵, M. Jablonski ², B. Jacak ⁷⁴, N. Jacazio ²⁶, P.M. Jacobs ⁷⁴, S. Jadlovská ¹⁰⁶, J. Jadlovský ¹⁰⁶, S. Jaelani ⁸², C. Jahnke ¹¹¹, M.J. Jakubowska ¹³⁵, M.A. Janik ¹³⁵, T. Janson ⁷⁰, S. Ji ¹⁷, S. Jia ¹⁰, A.A.P. Jimenez ⁶⁵, F. Jonas ⁸⁷, D.M. Jones ¹¹⁸, J.M. Jowett ^{33,97}, J. Jung ⁶⁴, M. Jung ⁶⁴, A. Junique ³³, A. Jusko ¹⁰⁰, M.J. Kabus ^{33,135}, J. Kaewjai ¹⁰⁵, P. Kalinak ⁶⁰, A.S. Kalteyer ⁹⁷, A. Kalweit ³³, V. Kaplin ¹⁴², A. Karasu Uysal ⁷², D. Karatovic ⁸⁹, O. Karavichev ¹⁴², T. Karavicheva ¹⁴², P. Karczmarczyk ¹³⁵, E. Karpechev ¹⁴², U. Kebschull ⁷⁰, R. Keidel ¹⁴¹, D.L.D. Keijdener ⁵⁹, M. Keil ³³, B. Ketzer ⁴³, S.S. Khade ⁴⁸, A.M. Khan ^{119,6}, S. Khan ¹⁶, A. Khanzadeev ¹⁴², Y. Kharlov ¹⁴², A. Khatun ¹¹⁷, A. Khuntia ³⁶, B. Kileng ³⁵, B. Kim ¹⁰⁴, C. Kim ¹⁷, D.J. Kim ¹¹⁶, E.J. Kim ⁶⁹, J. Kim ¹⁴⁰, J.S. Kim ⁴¹, J. Kim ⁵⁸, J. Kim ⁶⁹, M. Kim ¹⁹, S. Kim ¹⁸, T. Kim ¹⁴⁰, K. Kimura ⁹², S. Kirsch ⁶⁴, I. Kisel ³⁹, S. Kiselev ¹⁴², A. Kisiel ¹³⁵, J.P. Kitowski ², J.L. Klay ⁵, J. Klein ³³, S. Klein ⁷⁴, C. Klein-Bösing ¹³⁷, M. Kleiner ⁶⁴, T. Klemenz ⁹⁵, A. Kluge ³³, A.G. Knospe ¹¹⁵, C. Kobdaj ¹⁰⁵, T. Kollegger ⁹⁷, A. Kondratyev ¹⁴³, N. Kondratyeva ¹⁴², E. Kondratyuk ¹⁴², J. Konig ⁶⁴, S.A. Konigstorfer ⁹⁵, P.J. Konopka ³³, G. Kornakov ¹³⁵, S.D. Koryciak ², A. Kotliarov ⁸⁶, V. Kovalenko ¹⁴², M. Kowalski ¹⁰⁷, V. Kozhuharov ³⁷, I. Králík ⁶⁰, A. Kravčáková ³⁸, L. Krcal ^{33,39}, M. Krivda ^{100,60}, F. Krizek ⁸⁶, K. Krizkova Gajdosova ³³, M. Kroesen ⁹⁴, M. Krüger ⁶⁴, D.M. Krupova ³⁶, E. Kryshen ¹⁴², V. Kučera ⁵⁸, C. Kuhn ¹²⁸, P.G. Kuijer ⁸⁴, T. Kumaoka ¹²⁴, D. Kumar ¹³⁴, L. Kumar ⁹⁰, N. Kumar ⁹⁰, S. Kumar ³², S. Kundu ³³, P. Kurashvili ⁷⁹, A. Kurepin ¹⁴², A.B. Kurepin ¹⁴², A. Kuryakin ¹⁴², S. Kushpil ⁸⁶, M.J. Kweon ⁵⁸, Y. Kwon ¹⁴⁰, S.L. La Pointe ³⁹, P. La Rocca ²⁷, A. Lakerathok ¹⁰⁵, M. Lamanna ³³, R. Langoy ¹²⁰, P. Larionov ³³, E. Laudi ³³, L. Lautner ^{33,95}, R. Lavicka ¹⁰², R. Lea ^{133,55}, H. Lee ¹⁰⁴, I. Legrand ⁴⁶, G. Legras ¹³⁷, J. Lehrbach ³⁹, T.M. Lelek ², R.C. Lemmon ⁸⁵, I. León Monzón ¹⁰⁹, M.M. Lesch ⁹⁵, E.D. Lesser ¹⁹, P. Lévai ¹³⁸, X. Li ¹⁰, J. Lien ¹²⁰, R. Lietava ¹⁰⁰, I. Likmeta ¹¹⁵, B. Lim ²⁵, S.H. Lim ¹⁷, V. Lindenstruth ³⁹, A. Lindner ⁴⁶, C. Lippmann ⁹⁷, D.H. Liu ⁶, J. Liu ¹¹⁸, G.S.S. Liveraro ¹¹¹, I.M. Lofnes ²¹, C. Loizides ⁸⁷, S. Lokos ¹⁰⁷, J. Lomker ⁵⁹, P. Loncar ³⁴, X. Lopez ¹²⁶, E. López Torres ⁷, P. Lu ^{97,119}, J.R. Luhder ¹³⁷, M. Lunardon ²⁸, G. Luparello ⁵⁷, Y.G. Ma ⁴⁰, M. Mager ³³, A. Maire ¹²⁸, M.V. Makariev ³⁷, M. Malaev ¹⁴², G. Malfattore ²⁶, N.M. Malik ⁹¹, Q.W. Malik ²⁰, S.K. Malik ⁹¹, L. Malinina ^{VI,143}, D. Mallick ^{130,80}, N. Mallick ⁴⁸, G. Mandaglio ^{31,53}, S.K. Mandal ⁷⁹, V. Manko ¹⁴², F. Manso ¹²⁶, V. Manzari ⁵⁰, Y. Mao ⁶, R.W. Marcjan ², G.V. Margagliotti ²⁴, A. Margotti ⁵¹, A. Marín ⁹⁷, C. Markert ¹⁰⁸, P. Martinengo ³³, M.I. Martínez ⁴⁵, G. Martínez García ¹⁰³, M.P.P. Martins ¹¹⁰, S. Masciocchi ⁹⁷, M. Masera ²⁵, A. Masoni ⁵², L. Massacrier ¹³⁰, O. Massen ⁵⁹, A. Mastroserio ^{131,50}, O. Matonoha ⁷⁵, S. Mattiazzo ²⁸, A. Matyja ¹⁰⁷, C. Mayer ¹⁰⁷, A.L. Mazuecos ³³, F. Mazzaschi ²⁵, M. Mazzilli ³³, J.E. Mdhluli ¹²², Y. Melikyan ⁴⁴, A. Menchaca-Rocha ⁶⁷, E. Meninno ^{102,29}, A.S. Menon ¹¹⁵, M. Meres ¹³, S. Mhlanga ^{113,68}, Y. Miake ¹²⁴, L. Micheletti ³³, D.L. Mihaylov ⁹⁵, K. Mikhaylov ^{143,142}, A.N. Mishra ¹³⁸, D. Miśkowiec ⁹⁷, A. Modak ⁴, B. Mohanty ⁸⁰, M. Mohisin Khan ^{IV,16}, M.A. Molander ⁴⁴, S. Monira ¹³⁵, C. Mordasini ¹¹⁶, D.A. Moreira De Godoy ¹³⁷, I. Morozov ¹⁴², A. Morsch ³³, T. Mrnjavac ³³, V. Muccifora ⁴⁹, S. Muhuri ¹³⁴, J.D. Mulligan ⁷⁴, A. Mulliri ²³, M.G. Munhoz ¹¹⁰, R.H. Munzer ⁶⁴, H. Murakami ¹²³, S. Murray ¹¹³, L. Musa ³³, J. Musinsky ⁶⁰, J.W. Myrcha ¹³⁵, B. Naik ¹²², A.I. Nambrath ¹⁹, B.K. Nandi ⁴⁷, R. Nania ⁵¹, E. Nappi ⁵⁰, A.F. Nassirpour ¹⁸, A. Nath ⁹⁴, C. Nattrass ¹²¹, M.N. Naydenov ³⁷, A. Neagu ²⁰, A. Negru ¹²⁵, L. Nellen ⁶⁵, R. Nepeivoda ⁷⁵, S. Nese ²⁰, G. Neskovic ³⁹, N. Nicassio ⁵⁰, B.S. Nielsen ⁸³, E.G. Nielsen ⁸³, S. Nikolaev ¹⁴², S. Nikulin ¹⁴², V. Nikulin ¹⁴², F. Noferini ⁵¹, S. Noh ¹², P. Nomokonov ¹⁴³, J. Norman ¹¹⁸, N. Novitzky ¹²⁴, P. Nowakowski ¹³⁵, A. Nyanyan ¹⁴², J. Nystrand ²¹, M. Ogino ⁷⁶, S. Oh ¹⁸, A. Ohlson ⁷⁵, V.A. Okorokov ¹⁴², J. Oleniacz ¹³⁵, A.C. Oliveira Da Silva ¹²¹, A. Onnerstad ¹¹⁶, C. Oppedisano ⁵⁶, A. Ortiz Velasquez ⁶⁵, J. Otwinowski ¹⁰⁷, M. Oya ⁹², K. Oyama ⁷⁶, Y. Pachmayer ⁹⁴, S. Padhan ⁴⁷, D. Pagano ^{133,55}, G. Paić ⁶⁵, A. Palasciano ⁵⁰, S. Panebianco ¹²⁹, H. Park ¹²⁴, H. Park ¹⁰⁴, J. Park ⁵⁸, J.E. Parkkila ³³,

- Y. Patley ⁴⁷, R.N. Patra⁹¹, B. Paul ²³, H. Pei ⁶, T. Peitzmann ⁵⁹, X. Peng ¹¹, M. Pennisi ²⁵,
 S. Perciballi ²⁵, D. Peresunko ¹⁴², G.M. Perez ⁷, Y. Pestov¹⁴², V. Petrov ¹⁴², M. Petrovici ⁴⁶,
 R.P. Pezzi ^{103,66}, S. Piano ⁵⁷, M. Píkna ¹³, P. Pillot ¹⁰³, O. Pinazza ^{51,33}, L. Pinsky¹¹⁵, C. Pinto ⁹⁵,
 S. Pisano ⁴⁹, M. Płoskoń ⁷⁴, M. Planinic⁸⁹, F. Pliquet⁶⁴, M.G. Poghosyan ⁸⁷, B. Polichtchouk ¹⁴²,
 S. Politano ³⁰, N. Poljak ⁸⁹, A. Pop ⁴⁶, S. Porteboeuf-Houssais ¹²⁶, V. Pozdniakov ¹⁴³, I.Y. Pozos ⁴⁵,
 K.K. Pradhan ⁴⁸, S.K. Prasad ⁴, S. Prasad ⁴⁸, R. Preghenella ⁵¹, F. Prino ⁵⁶, C.A. Pruneau ¹³⁶,
 I. Pshenichnov ¹⁴², M. Puccio ³³, S. Pucillo ²⁵, Z. Pugelova¹⁰⁶, S. Qiu ⁸⁴, L. Quaglia ²⁵, S. Ragoni ¹⁵,
 A. Rai ¹³⁹, A. Rakotozafindrabe ¹²⁹, L. Ramello ^{132,56}, F. Rami ¹²⁸, S.A.R. Ramirez ⁴⁵, T.A. Rancien⁷³,
 M. Rasa ²⁷, S.S. Räsänen ⁴⁴, R. Rath ⁵¹, M.P. Rauch ²¹, I. Ravasenga ⁸⁴, K.F. Read ^{87,121},
 C. Reckziegel ¹¹², A.R. Redelbach ³⁹, K. Redlich ^{V,79}, C.A. Reetz ⁹⁷, A. Rehman²¹, F. Reidt ³³,
 H.A. Reme-Ness ³⁵, Z. Rescakova³⁸, K. Reygers ⁹⁴, A. Riabov ¹⁴², V. Riabov ¹⁴², R. Ricci ²⁹,
 M. Richter ²⁰, A.A. Riedel ⁹⁵, W. Riegler ³³, A.G. Riffero ²⁵, C. Ristea ⁶³, M.V. Rodriguez ³³,
 M. Rodríguez Cahuantzi ⁴⁵, K. Røed ²⁰, R. Rogalev ¹⁴², E. Rogochaya ¹⁴³, T.S. Rogoschinski ⁶⁴,
 D. Rohr ³³, D. Röhrich ²¹, P.F. Rojas⁴⁵, S. Rojas Torres ³⁶, P.S. Rokita ¹³⁵, G. Romanenko ²⁶,
 F. Ronchetti ⁴⁹, A. Rosano ^{31,53}, E.D. Rosas⁶⁵, K. Roslon ¹³⁵, A. Rossi ⁵⁴, A. Roy ⁴⁸, S. Roy ⁴⁷,
 N. Rubini ²⁶, O.V. Rueda ¹¹⁵, D. Ruggiano ¹³⁵, R. Rui ²⁴, P.G. Russek ², R. Russo ⁸⁴,
 A. Rustamov ⁸¹, E. Ryabinkin ¹⁴², Y. Ryabov ¹⁴², A. Rybicki ¹⁰⁷, H. Rytkonen ¹¹⁶, J. Ryu ¹⁷,
 W. Rzesz ¹³⁵, O.A.M. Saarimaki ⁴⁴, S. Sadhu ³², S. Sadovsky ¹⁴², J. Saetre ²¹, K. Šafařík ³⁶, P. Saha⁴²,
 S.K. Saha ⁴, S. Saha ⁸⁰, B. Sahoo ⁴⁷, B. Sahoo ⁴⁸, R. Sahoo⁶¹, D. Sahu ⁴⁸, P.K. Sahu ⁶¹,
 J. Saini ¹³⁴, K. Sajdakova³⁸, S. Sakai ¹²⁴, M.P. Salvan ⁹⁷, S. Sambyal ⁹¹, D. Samitz ¹⁰², I. Sanna ^{33,95},
 T.B. Saramela¹¹⁰, P. Sarma ⁴², V. Sarritzu ²³, V.M. Sarti ⁹⁵, M.H.P. Sas ¹³⁹, J. Schambach ⁸⁷,
 H.S. Scheid ⁶⁴, C. Schiaua ⁴⁶, R. Schicker ⁹⁴, A. Schmah⁹⁷, C. Schmidt ⁹⁷, H.R. Schmidt⁹³,
 M.O. Schmidt ³³, M. Schmidt⁹³, N.V. Schmidt ⁸⁷, A.R. Schmier ¹²¹, R. Schotter ¹²⁸, A. Schröter ³⁹,
 J. Schukraft ³³, K. Schweda ⁹⁷, G. Scioli ²⁶, E. Scomparin ⁵⁶, J.E. Seger ¹⁵, Y. Sekiguchi¹²³,
 D. Sekihata ¹²³, M. Selina ⁸⁴, I. Selyuzhenkov ⁹⁷, S. Senyukov ¹²⁸, J.J. Seo ^{94,58}, D. Serebryakov ¹⁴²,
 L. Šerkšnytė ⁹⁵, A. Sevcenco ⁶³, T.J. Shaba ⁶⁸, A. Shabetai ¹⁰³, R. Shahoyan³³, A. Shangaraev ¹⁴²,
 A. Sharma⁹⁰, B. Sharma ⁹¹, D. Sharma ⁴⁷, H. Sharma ^{54,107}, M. Sharma ⁹¹, S. Sharma ⁷⁶, S. Sharma ⁹¹,
 U. Sharma ⁹¹, A. Shatat ¹³⁰, O. Sheibani¹¹⁵, K. Shigaki ⁹², M. Shimomura⁷⁷, J. Shin¹², S. Shirinkin ¹⁴²,
 Q. Shou ⁴⁰, Y. Sibirjak ¹⁴², S. Siddhanta ⁵², T. Siemianczuk ⁷⁹, T.F. Silva ¹¹⁰, D. Silvermyr ⁷⁵,
 T. Simantathammakul¹⁰⁵, R. Simeonov ³⁷, B. Singh⁹¹, B. Singh ⁹⁵, K. Singh ⁴⁸, R. Singh ⁸⁰,
 R. Singh ⁹¹, R. Singh ⁴⁸, S. Singh ¹⁶, V.K. Singh ¹³⁴, V. Singhal ¹³⁴, T. Sinha ⁹⁹, B. Sitar ¹³,
 M. Sitta ^{132,56}, T.B. Skaali²⁰, G. Skorodumovs ⁹⁴, M. Slupecki ⁴⁴, N. Smirnov ¹³⁹, R.J.M. Snellings ⁵⁹,
 E.H. Solheim ²⁰, J. Song ¹¹⁵, C. Sonnabend ^{33,97}, F. Soramel ²⁸, A.B. Soto-hernandez ⁸⁸,
 R. Spijkers ⁸⁴, I. Sputowska ¹⁰⁷, J. Staa ⁷⁵, J. Stachel ⁹⁴, I. Stan ⁶³, P.J. Steffanic ¹²¹,
 S.F. Stiefelmaier ⁹⁴, D. Stocco ¹⁰³, I. Storehaug ²⁰, P. Stratmann ¹³⁷, S. Strazzi ²⁶, A. Sturniolo ^{31,53},
 C.P. Stylianidis⁸⁴, A.A.P. Suaide ¹¹⁰, C. Suire ¹³⁰, M. Sukhanov ¹⁴², M. Suljic ³³, R. Sultanov ¹⁴²,
 V. Sumberia ⁹¹, S. Sumowidagdo ⁸², S. Swain⁶¹, I. Szarka ¹³, M. Szymkowski ¹³⁵, S.F. Taghavi ⁹⁵,
 G. Taillepied ⁹⁷, J. Takahashi ¹¹¹, G.J. Tambave ⁸⁰, S. Tang ⁶, Z. Tang ¹¹⁹, J.D. Tapia Takaki ¹¹⁷,
 N. Tapus¹²⁵, L.A. Tarasovicova ¹³⁷, M.G. Tarzila ⁴⁶, G.F. Tassielli ³², A. Tauro ³³, G. Tejeda Muñoz ⁴⁵,
 A. Telesca ³³, L. Terlizzi ²⁵, C. Terrevoli ¹¹⁵, S. Thakur ⁴, D. Thomas ¹⁰⁸, A. Tikhonov ¹⁴²,
 A.R. Timmins ¹¹⁵, M. Tkacik¹⁰⁶, T. Tkacik ¹⁰⁶, A. Toia ⁶⁴, R. Tokumoto⁹², K. Tomohiro⁹²,
 N. Topilskaya ¹⁴², M. Toppi ⁴⁹, T. Tork ¹³⁰, V.V. Torres ¹⁰³, A.G. Torres Ramos ³², A. Trifiró ^{31,53},
 A.S. Triolo ^{33,31,53}, S. Tripathy ⁵¹, T. Tripathy ⁴⁷, S. Trogolo ³³, V. Trubnikov ³, W.H. Trzaska ¹¹⁶,
 T.P. Trzcinski ¹³⁵, A. Tumkin ¹⁴², R. Turrisi ⁵⁴, T.S. Tveter ²⁰, K. Ullaland ²¹, B. Ulukutlu ⁹⁵,
 A. Uras ¹²⁷, G.L. Usai ²³, M. Vala³⁸, N. Valle ²², L.V.R. van Doremalen⁵⁹, M. van Leeuwen ⁸⁴, C.A. van
 Veen ⁹⁴, R.J.G. van Weelden ⁸⁴, P. Vande Vyvre ³³, D. Varga ¹³⁸, Z. Varga ¹³⁸, M. Vasileiou ⁷⁸,
 A. Vasiliev ¹⁴², O. Vázquez Doce ⁴⁹, V. Vechernin ¹⁴², E. Vercellin ²⁵, S. Vergara Limón⁴⁵, R. Verma⁴⁷,
 L. Vermunt ⁹⁷, R. Vértesi ¹³⁸, M. Verweij ⁵⁹, L. Vickovic³⁴, Z. Vilakazi¹²², O. Villalobos Baillie ¹⁰⁰,
 A. Villani ²⁴, A. Vinogradov ¹⁴², T. Virgili ²⁹, M.M.O. Virta ¹¹⁶, V. Vislavicius⁷⁵, A. Vodopyanov ¹⁴³,
 B. Volkel ³³, M.A. Völk ⁹⁴, K. Voloshin¹⁴², S.A. Voloshin ¹³⁶, G. Volpe ³², B. von Haller ³³,
 I. Vorobyev ⁹⁵, N. Vozniuk ¹⁴², J. Vrláková ³⁸, J. Wan⁴⁰, C. Wang ⁴⁰, D. Wang ⁴⁰, Y. Wang ⁴⁰,
 Y. Wang ⁶, A. Wegrzynek ³³, F.T. Weighofer³⁹, S.C. Wenzel ³³, J.P. Wessels ¹³⁷, S.L. Weyhmiller ¹³⁹,
 J. Wiechula ⁶⁴, J. Wikne ²⁰, G. Wilk ⁷⁹, J. Wilkinson ⁹⁷, G.A. Willems ¹³⁷, B. Windelband ⁹⁴,
 M. Winn ¹²⁹, J.R. Wright ¹⁰⁸, W. Wu⁴⁰, Y. Wu ¹¹⁹, R. Xu ⁶, A. Yadav ⁴³, A.K. Yadav ¹³⁴,
 S. Yalcin ⁷², Y. Yamaguchi ⁹², S. Yang²¹, S. Yano ⁹², Z. Yin ⁶, I.-K. Yoo ¹⁷, J.H. Yoon ⁵⁸, H. Yu¹²,
 S. Yuan²¹, A. Yuncu ⁹⁴, V. Zaccolo ²⁴, C. Zampolli ³³, F. Zanone ⁹⁴, N. Zardoshti ³³,

A. Zarochentsev ¹⁴², P. Závada ⁶², N. Zaviyalov ¹⁴², M. Zhalov ¹⁴², B. Zhang ⁶, C. Zhang ¹²⁹, L. Zhang ⁴⁰, S. Zhang ⁴⁰, X. Zhang ⁶, Y. Zhang ¹¹⁹, Z. Zhang ⁶, M. Zhao ¹⁰, V. Zherebchevskii ¹⁴², Y. Zhi ¹⁰, D. Zhou ⁶, Y. Zhou ⁸³, J. Zhu ^{54,6}, Y. Zhu ⁶, S.C. Zugravil ⁵⁶, N. Zurlo ^{133,55}

Affiliation Notes

^I Also at: Max-Planck-Institut für Physik, Munich, Germany

^{II} Also at: Italian National Agency for New Technologies, Energy and Sustainable Economic Development (ENEA), Bologna, Italy

^{III} Also at: Dipartimento DET del Politecnico di Torino, Turin, Italy

^{IV} Also at: Department of Applied Physics, Aligarh Muslim University, Aligarh, India

^V Also at: Institute of Theoretical Physics, University of Wroclaw, Poland

^{VI} Also at: An institution covered by a cooperation agreement with CERN

Collaboration Institutes

¹ A.I. Alikhanyan National Science Laboratory (Yerevan Physics Institute) Foundation, Yerevan, Armenia

² AGH University of Science and Technology, Cracow, Poland

³ Bogolyubov Institute for Theoretical Physics, National Academy of Sciences of Ukraine, Kiev, Ukraine

⁴ Bose Institute, Department of Physics and Centre for Astroparticle Physics and Space Science (CAPSS), Kolkata, India

⁵ California Polytechnic State University, San Luis Obispo, California, United States

⁶ Central China Normal University, Wuhan, China

⁷ Centro de Aplicaciones Tecnológicas y Desarrollo Nuclear (CEADEN), Havana, Cuba

⁸ Centro de Investigación y de Estudios Avanzados (CINVESTAV), Mexico City and Mérida, Mexico

⁹ Chicago State University, Chicago, Illinois, United States

¹⁰ China Institute of Atomic Energy, Beijing, China

¹¹ China University of Geosciences, Wuhan, China

¹² Chungbuk National University, Cheongju, Republic of Korea

¹³ Comenius University Bratislava, Faculty of Mathematics, Physics and Informatics, Bratislava, Slovak Republic

¹⁴ COMSATS University Islamabad, Islamabad, Pakistan

¹⁵ Creighton University, Omaha, Nebraska, United States

¹⁶ Department of Physics, Aligarh Muslim University, Aligarh, India

¹⁷ Department of Physics, Pusan National University, Pusan, Republic of Korea

¹⁸ Department of Physics, Sejong University, Seoul, Republic of Korea

¹⁹ Department of Physics, University of California, Berkeley, California, United States

²⁰ Department of Physics, University of Oslo, Oslo, Norway

²¹ Department of Physics and Technology, University of Bergen, Bergen, Norway

²² Dipartimento di Fisica, Università di Pavia, Pavia, Italy

²³ Dipartimento di Fisica dell’Università and Sezione INFN, Cagliari, Italy

²⁴ Dipartimento di Fisica dell’Università and Sezione INFN, Trieste, Italy

²⁵ Dipartimento di Fisica dell’Università and Sezione INFN, Turin, Italy

²⁶ Dipartimento di Fisica e Astronomia dell’Università and Sezione INFN, Bologna, Italy

²⁷ Dipartimento di Fisica e Astronomia dell’Università and Sezione INFN, Catania, Italy

²⁸ Dipartimento di Fisica e Astronomia dell’Università and Sezione INFN, Padova, Italy

²⁹ Dipartimento di Fisica ‘E.R. Caianiello’ dell’Università and Gruppo Collegato INFN, Salerno, Italy

³⁰ Dipartimento DISAT del Politecnico and Sezione INFN, Turin, Italy

³¹ Dipartimento di Scienze MIFT, Università di Messina, Messina, Italy

³² Dipartimento Interateneo di Fisica ‘M. Merlin’ and Sezione INFN, Bari, Italy

³³ European Organization for Nuclear Research (CERN), Geneva, Switzerland

³⁴ Faculty of Electrical Engineering, Mechanical Engineering and Naval Architecture, University of Split, Split, Croatia

³⁵ Faculty of Engineering and Science, Western Norway University of Applied Sciences, Bergen, Norway

³⁶ Faculty of Nuclear Sciences and Physical Engineering, Czech Technical University in Prague, Prague, Czech Republic

³⁷ Faculty of Physics, Sofia University, Sofia, Bulgaria

- ³⁸ Faculty of Science, P.J. Šafárik University, Košice, Slovak Republic
³⁹ Frankfurt Institute for Advanced Studies, Johann Wolfgang Goethe-Universität Frankfurt, Frankfurt, Germany
⁴⁰ Fudan University, Shanghai, China
⁴¹ Gangneung-Wonju National University, Gangneung, Republic of Korea
⁴² Gauhati University, Department of Physics, Guwahati, India
⁴³ Helmholtz-Institut für Strahlen- und Kernphysik, Rheinische Friedrich-Wilhelms-Universität Bonn, Bonn, Germany
⁴⁴ Helsinki Institute of Physics (HIP), Helsinki, Finland
⁴⁵ High Energy Physics Group, Universidad Autónoma de Puebla, Puebla, Mexico
⁴⁶ Horia Hulubei National Institute of Physics and Nuclear Engineering, Bucharest, Romania
⁴⁷ Indian Institute of Technology Bombay (IIT), Mumbai, India
⁴⁸ Indian Institute of Technology Indore, Indore, India
⁴⁹ INFN, Laboratori Nazionali di Frascati, Frascati, Italy
⁵⁰ INFN, Sezione di Bari, Bari, Italy
⁵¹ INFN, Sezione di Bologna, Bologna, Italy
⁵² INFN, Sezione di Cagliari, Cagliari, Italy
⁵³ INFN, Sezione di Catania, Catania, Italy
⁵⁴ INFN, Sezione di Padova, Padova, Italy
⁵⁵ INFN, Sezione di Pavia, Pavia, Italy
⁵⁶ INFN, Sezione di Torino, Turin, Italy
⁵⁷ INFN, Sezione di Trieste, Trieste, Italy
⁵⁸ Inha University, Incheon, Republic of Korea
⁵⁹ Institute for Gravitational and Subatomic Physics (GRASP), Utrecht University/Nikhef, Utrecht, Netherlands
⁶⁰ Institute of Experimental Physics, Slovak Academy of Sciences, Košice, Slovak Republic
⁶¹ Institute of Physics, Homi Bhabha National Institute, Bhubaneswar, India
⁶² Institute of Physics of the Czech Academy of Sciences, Prague, Czech Republic
⁶³ Institute of Space Science (ISS), Bucharest, Romania
⁶⁴ Institut für Kernphysik, Johann Wolfgang Goethe-Universität Frankfurt, Frankfurt, Germany
⁶⁵ Instituto de Ciencias Nucleares, Universidad Nacional Autónoma de México, Mexico City, Mexico
⁶⁶ Instituto de Física, Universidade Federal do Rio Grande do Sul (UFRGS), Porto Alegre, Brazil
⁶⁷ Instituto de Física, Universidad Nacional Autónoma de México, Mexico City, Mexico
⁶⁸ iThemba LABS, National Research Foundation, Somerset West, South Africa
⁶⁹ Jeonbuk National University, Jeonju, Republic of Korea
⁷⁰ Johann-Wolfgang-Goethe Universität Frankfurt Institut für Informatik, Fachbereich Informatik und Mathematik, Frankfurt, Germany
⁷¹ Korea Institute of Science and Technology Information, Daejeon, Republic of Korea
⁷² KTO Karatay University, Konya, Turkey
⁷³ Laboratoire de Physique Subatomique et de Cosmologie, Université Grenoble-Alpes, CNRS-IN2P3, Grenoble, France
⁷⁴ Lawrence Berkeley National Laboratory, Berkeley, California, United States
⁷⁵ Lund University Department of Physics, Division of Particle Physics, Lund, Sweden
⁷⁶ Nagasaki Institute of Applied Science, Nagasaki, Japan
⁷⁷ Nara Women's University (NWU), Nara, Japan
⁷⁸ National and Kapodistrian University of Athens, School of Science, Department of Physics , Athens, Greece
⁷⁹ National Centre for Nuclear Research, Warsaw, Poland
⁸⁰ National Institute of Science Education and Research, Homi Bhabha National Institute, Jatni, India
⁸¹ National Nuclear Research Center, Baku, Azerbaijan
⁸² National Research and Innovation Agency - BRIN, Jakarta, Indonesia
⁸³ Niels Bohr Institute, University of Copenhagen, Copenhagen, Denmark
⁸⁴ Nikhef, National institute for subatomic physics, Amsterdam, Netherlands
⁸⁵ Nuclear Physics Group, STFC Daresbury Laboratory, Daresbury, United Kingdom
⁸⁶ Nuclear Physics Institute of the Czech Academy of Sciences, Husinec-Řež, Czech Republic
⁸⁷ Oak Ridge National Laboratory, Oak Ridge, Tennessee, United States
⁸⁸ Ohio State University, Columbus, Ohio, United States
⁸⁹ Physics department, Faculty of science, University of Zagreb, Zagreb, Croatia
⁹⁰ Physics Department, Panjab University, Chandigarh, India

- ⁹¹ Physics Department, University of Jammu, Jammu, India
⁹² Physics Program and International Institute for Sustainability with Knotted Chiral Meta Matter (SKCM2), Hiroshima University, Hiroshima, Japan
⁹³ Physikalisches Institut, Eberhard-Karls-Universität Tübingen, Tübingen, Germany
⁹⁴ Physikalisches Institut, Ruprecht-Karls-Universität Heidelberg, Heidelberg, Germany
⁹⁵ Physik Department, Technische Universität München, Munich, Germany
⁹⁶ Politecnico di Bari and Sezione INFN, Bari, Italy
⁹⁷ Research Division and ExtreMe Matter Institute EMMI, GSI Helmholtzzentrum für Schwerionenforschung GmbH, Darmstadt, Germany
⁹⁸ Saga University, Saga, Japan
⁹⁹ Saha Institute of Nuclear Physics, Homi Bhabha National Institute, Kolkata, India
¹⁰⁰ School of Physics and Astronomy, University of Birmingham, Birmingham, United Kingdom
¹⁰¹ Sección Física, Departamento de Ciencias, Pontificia Universidad Católica del Perú, Lima, Peru
¹⁰² Stefan Meyer Institut für Subatomare Physik (SMI), Vienna, Austria
¹⁰³ SUBATECH, IMT Atlantique, Nantes Université, CNRS-IN2P3, Nantes, France
¹⁰⁴ Sungkyunkwan University, Suwon City, Republic of Korea
¹⁰⁵ Suranaree University of Technology, Nakhon Ratchasima, Thailand
¹⁰⁶ Technical University of Košice, Košice, Slovak Republic
¹⁰⁷ The Henryk Niewodniczanski Institute of Nuclear Physics, Polish Academy of Sciences, Cracow, Poland
¹⁰⁸ The University of Texas at Austin, Austin, Texas, United States
¹⁰⁹ Universidad Autónoma de Sinaloa, Culiacán, Mexico
¹¹⁰ Universidade de São Paulo (USP), São Paulo, Brazil
¹¹¹ Universidade Estadual de Campinas (UNICAMP), Campinas, Brazil
¹¹² Universidade Federal do ABC, Santo Andre, Brazil
¹¹³ University of Cape Town, Cape Town, South Africa
¹¹⁴ University of Derby, Derby, United Kingdom
¹¹⁵ University of Houston, Houston, Texas, United States
¹¹⁶ University of Jyväskylä, Jyväskylä, Finland
¹¹⁷ University of Kansas, Lawrence, Kansas, United States
¹¹⁸ University of Liverpool, Liverpool, United Kingdom
¹¹⁹ University of Science and Technology of China, Hefei, China
¹²⁰ University of South-Eastern Norway, Kongsberg, Norway
¹²¹ University of Tennessee, Knoxville, Tennessee, United States
¹²² University of the Witwatersrand, Johannesburg, South Africa
¹²³ University of Tokyo, Tokyo, Japan
¹²⁴ University of Tsukuba, Tsukuba, Japan
¹²⁵ University Politehnica of Bucharest, Bucharest, Romania
¹²⁶ Université Clermont Auvergne, CNRS/IN2P3, LPC, Clermont-Ferrand, France
¹²⁷ Université de Lyon, CNRS/IN2P3, Institut de Physique des 2 Infinis de Lyon, Lyon, France
¹²⁸ Université de Strasbourg, CNRS, IPHC UMR 7178, F-67000 Strasbourg, France, Strasbourg, France
¹²⁹ Université Paris-Saclay, Centre d'Etudes de Saclay (CEA), IRFU, Département de Physique Nucléaire (DPhN), Saclay, France
¹³⁰ Université Paris-Saclay, CNRS/IN2P3, IJCLab, Orsay, France
¹³¹ Università degli Studi di Foggia, Foggia, Italy
¹³² Università del Piemonte Orientale, Vercelli, Italy
¹³³ Università di Brescia, Brescia, Italy
¹³⁴ Variable Energy Cyclotron Centre, Homi Bhabha National Institute, Kolkata, India
¹³⁵ Warsaw University of Technology, Warsaw, Poland
¹³⁶ Wayne State University, Detroit, Michigan, United States
¹³⁷ Westfälische Wilhelms-Universität Münster, Institut für Kernphysik, Münster, Germany
¹³⁸ Wigner Research Centre for Physics, Budapest, Hungary
¹³⁹ Yale University, New Haven, Connecticut, United States
¹⁴⁰ Yonsei University, Seoul, Republic of Korea
¹⁴¹ Zentrum für Technologie und Transfer (ZTT), Worms, Germany
¹⁴² Affiliated with an institute covered by a cooperation agreement with CERN
¹⁴³ Affiliated with an international laboratory covered by a cooperation agreement with CERN.